patients with type 2 DM. In the present study, we investigated whether increased adiponectin levels are associated with hippocampus volume and insulin resistance in patients with type 2 DM.

2. Subjects and methods

2.1. Subjects

We screened patients seen at the Department of Endocrinology of Oita Red Cross Hospital between Jun 2008 and Jun 2010 for the treatment of type 2 DM, detected by medical examination. Of these patients, 45 Japanese men aged between 50 and 75 years (mean (SD) age 65 ± 8 years) fulfilled the inclusion criteria and were enrolled in the present study. All subjects gave written informed consent to participate in the study. The study protocol was approved by the ethics committee of Oita Red Cross Hospital.

2.2. Assays

Blood was extracted from the antecubital vein from patients in the recumbent position at 7:00 am after an overnight fast. All patients underwent routine laboratory tests, including assays for serum electrolytes, total cholesterol, triglycerides, high-density lipoprotein cholesterol (HDL-C), low-density lipoprotein cholesterol (LDL-C), fasting serum glucose (FSG), and fasting immunoreactive insulin (F-IRI). Insulin resistance was evaluated by the homeostasis model assessment (HOMA) index, calculated as fasting serum insulin (μU/mL) × fasting serum glucose (mmol/L) / 22.5 [15]. The concentrations of total adiponectin, including trimers, hexamers and a high-molecular weight form, were measured using a commercially available enzyme-linked immunosorbent assay kit (Otsuka Pharmaceuticals, Tokyo, Japan). The serum adiponectin cutoff was 4.0 μg/mL, a value that has been used previously [16].

2.3. Cognitive performance

Cognitive function was measured using the mini-mental state examination (MMSE) [17], a 23-item global cognitive function test that includes questions on orientation in time and place, attention, language, memory and visual construction. Scores range from 0 to 30, and the cutoff value of 27 suggests mild impairment of cognition.

2.4. Voxel-based analysis

Running on Windows XP, VSRAD compares the gray matter image of an individual patient to the mean (SD) gray matter images using voxel-by-voxel Z-score analysis after voxel normalization to global mean intensities in the same manner as is implemented in the easy Z-score imaging system. A group of aged-matched healthy subjects was selected for each group of patients in this study. The control subjects did not have DM, showed no clinical evidence of cognitive deficits or neurologic disease, and were not receiving short- or long-term drug therapy at the time of imaging. They had no abnormal findings in their images, disregarding age-related atrophy and white matter changes in T2-weighted images. Each patient gray matter image was compared to the mean (SD) gray matter images using voxel-by-voxel Z-score analysis after voxel normalization to global mean intensities. The following formula was used: Z-score = (control mean − individual value) / (control SD). Z-score maps were displayed by overlaying on tomographic sections. VSRAD can automatically analyze the data as a series of segmentation, anatomical standardization and smoothing using SPM2 without a MATLAB program and performs Z-score analysis of the bilateral temporal areas [18,19].

2.5. Statistical analysis

Data are presented as the mean ± SD. Differences between the two groups were analyzed by unpaired Student's t test, chi-square test, or Fisher's exact probability test. A P value of $< .05$ was considered statistically significant. Simple (Spearman's rank) correlation coefficients were calculated for correlations between adiponectin and various parameters. Stepwise multiple regression analysis was performed.

3. Results

The mean ages of the patients with type 2 DM in the low and normal adiponectin groups were similar, and there were no significant differences between the groups with respect to duration of diabetes or administered medications. Body mass index (BMI) was higher in the low adiponectin group than in the normal adiponectin group. Resting heart rate and systolic and diastolic blood pressure did not differ significantly between the two groups.

Fasting serum glucose and insulin concentrations and HOMA index values were all higher in the low adiponectin group than in the normal adiponectin group. However, there was no significant difference in hemoglobin A1c percentage between the two groups. The serum concentrations of triglycerides and HDL-C were respectively higher and lower in the low adiponectin group, as compared to the normal adiponectin group. Serum total cholesterol, LDL-C and uric acid levels did not differ significantly between the two groups. Measures of renal function, including serum creatinine concentration, were similar in the two groups.

Cognitive performance, assessed by MMSE score, did not differ significantly between the two groups. However, hippocampus volume was lower in the low adiponectin group than in the normal adiponectin group ($P < .0001$).

Table 1 shows the correlations between adiponectin level and age, body mass index, and other variables in both groups. Adiponectin levels were negatively correlated with BMI, fasting serum glucose concentration, fasting serum insulin concentration, HOMA index value, and Z-score, but were positively correlated with HDL-C.

Multiple regression analysis was performed using a stepwise procedure. BMI, waist circumference, TGL, HDL-C, FSG, F-IRI, HOMA index and hippocampus atrophy were included as variables in the multiple regression analysis. The level of adiponectin was independently predicted by Z-score ($F = 16.974$) and HOMA index ($F = 22.109$) (Table 2).

Table 1 – Correlations between adiponectin and various parameters.

Parameters	Univariate analysis	
	R	P value
Age	−0.075	.6245
Duration of diabetes mellitus	−0.205	.1722
Body mass index	−0.430	.0032
Waist circumferences	0.366	.0104
Systolic blood pressure	−0.183	.2295
Diastolic blood pressure	−0.207	.1729
Heart rate	−0.111	.4681
Total cholesterol	−0.238	.1157
Triglyceride	−0.349	.0187
High-density lipoprotein cholesterol	0.339	.0225
Low-density lipoprotein cholesterol	−0.253	.0942
Uric acid	−0.254	.0924
Fasting serum glucose	−0.510	.0003
Fasting insulin	−0.615	<.0001
Homeostasis model assessment index	−0.671	<.0001
Hemoglobin A1c	−0.053	.7308
Creatinine	−0.066	.6673
MMSE	0.258	.0870
Hippocampus atrophy (Z-score)	−0.634	<.0001

MMSE = mini-mental status examination.

4. Discussion

Patients with type 2 DM with low adiponectin levels showed a decrease in hippocampus volume in the present study. Among the metabolic parameters we investigated, fasting serum concentrations of glucose and insulin and HOMA index were higher in patients with low adiponectin levels than in those with normal adiponectin levels. In addition, multiple regression analysis revealed that serum adiponectin levels in patients with type 2 DM could be independently predicted by HOMA index and hippocampus volume. It is possible that type 2 DM plus decreased adiponectin level is a predictor of hippocampus volume.

Several mechanisms could explain our observations. First, adiponectin has a neuroprotective effect on hippocampal neurons [20]. Treatment with adiponectin preserves the integrity of the blood–brain barrier and has a neuroprotective effect on hippocampal neurons [20]. Second, adiponectin plays a direct protective role against atherosclerotic vascular change, and loss of effects enhances endothelial dysfunction in the brain. Circulating adiponectin is strongly linked to protection against endothelial cell damage [8]. Third, adiponectin plays a role in the pathogenesis of multiple sclerosis and Alzheimer's disease [13,14]. Taken together, these findings suggest that the hippocampus and adiponectin interact and reinforce each other through mechanisms that may be associated with neuroprotective and vasculoprotective effects.

This study has several limitations. First, the number of patients was small. Large cohort studies including other populations may be beneficial for elucidating these relationships. Second, the Z-score-based neuroimaging method we used is not a standard method and it is unclear whether the Z-score can be directly translated into a measure of hippocampus volume without explicit anatomic segmentation of the MR images (as was performed in the present study). Other neuroimaging methods are needed to determine the relationships between adiponectin, metabolic parameters and hippocampus volume in the future.

In conclusion, our findings suggest that hypoadiponectinemia is associated with hippocampus volume.

Table 2 – Stepwise regression analysis between adiponectin and other parameters.

Independent variable	Regression coefficient	Standard error	Standard regression coefficient	F-value
To adiponectin intercept	13.211			
Hippocampus volume (Z-score)	−3.295	0.801	−0.435	16.974
HOMA index	−1.681	0.358	−0.496	22.109

HOMA = homeostasis model assessment.

Authors' Contribution

TM analyzed data and wrote and revised/edited manuscript; TM and FA provided patient care and samples, collected data, compiled database, and revised manuscript; TS, MF and TS supervised the overall study with HY, provided patient care and samples, and revised manuscript.

Funding

This work was supported by a grant from the Japanese Ministry of Education, Science and Culture and Research on Measures for Intractable Diseases, Japanese Ministry of Health, Welfare and Labor, Japan.

Conflict of interest

All authors have no conflicts of interest.

REFERENCES

[1] Goldstein LB, Adams R, Becker K. Primary prevention of ischemic stroke: a statement for healthcare professionals from the Stroke Council of the American Heart Association. Circulation 2001;103:163-82.
[2] Hébert R, Lindsay J, Verreault R, Rockwood K, Hill G, Dubois MF. Vascular dementia: incidence and risk factors in the Canadian study of health and aging. Stroke 2000;31:1487-93.
[3] Peila R, Rodriguez BL, Launer LJ. Honolulu–Asia Aging Study. Type 2 diabetes, APOE gene, and the risk for dementia and related pathologies: the Honolulu–Asia Aging Study. Diabetes 2000;51:1256-62.
[4] Ridgway GR, Henley SM, Fox NC, et al. Ten simple rules for reporting voxel-based morphometry studies. Neuroimage 2008;40:1429-35.

[5] Hirata Y, Matsuda H, Nemoto K. Voxel-based morphometry to discriminate early Alzheimer's disease from controls. Neurosci Lett 2005;382:269-74.
[6] Kadowaki T, Yamauchi T. Adiponectin and adiponectin receptors. Endocr Rev 2005;26:439-51.
[7] Matsuzawa Y. The metabolic syndrome and adipocytokines. FEBS Lett 2006;80:2917-21.
[8] Masaki T, Chiba S, Tatsukawa H. Adiponectin protects LPS-induced liver injury through modulation of TNF-alpha in KK-Ay obese mice. Hepatology 2004;40:177-84.
[9] Masaki T, Chiba S, Yasuda T. Peripheral, but not central, administration of adiponectin reduces visceral adiposity and upregulates the expression of uncoupling protein in agouti yellow (Ay/a) obese mice. Diabetes 2003;52:2266-73.
[10] Annuzzi G, Bozzetto L, Patti L, et al. Type 2 diabetes mellitus is characterized by reduced postprandial adiponectin response: a possible link with diabetic postprandial dyslipidemia. Metabolism 2010;59:567-74.
[11] Giannessi D, Caselli C, Del Ry S, et al. Adiponectin is associated with abnormal lipid profile and coronary microvascular dysfunction in patients with dilated cardiomyopathy without overt heart failure. Metabolism 2011;60: 227-33.
[12] Polyzos SA, Toulis KA, Goulis DG, Zavos C, Kountouras J. Serum total adiponectin in nonalcoholic fatty liver disease: a systematic review and meta-analysis. Metabolism 2011;60: 313-26.
[13] Musabak U, Demirkaya S, Genç G, Ilikci RS, Odabasi Z. Serum adiponectin, TNF-α, IL-12p70, and IL-13 levels in multiple sclerosis and the effects of different therapy regimens. Neuroimmunomodulation 2011;18:57-66.
[14] Une K, Takei YA, Tomita N, Asamura T, Ohrui T, Furukawa K, Arai H. Adiponectin in plasma and cerebrospinal fluid in MCI and Alzheimer's disease. Eur J Neurol 2011;18:1006-9.
[15] Matthews DR, Hosker JP, Rudenski AS, et al. Homeostasis model assessment: insulin resistance and beta-cell function from fasting plasma glucose and insulin concentrations in man. Diabetologia 1985;28:412-9.
[16] Kumada M, Kihara S, Sumitsuji S, et al. Association of hypoadiponectinemia with coronary artery disease in men. Arterioscler Thromb Vasc Biol 2003;23:85-9.
[17] Folstein MF, Folstein SE, McHugh PR. Mini-mental state. A practical method for grading the cognitive state of patients for the clinician. J Psychiatr Res 1975;12:189-98.
[18] Ashburner J Friston KJ. Voxel-based morphometry: the methods. NeuroImage 2000;11:805-21.
[19] Anan F, Masaki T, Shimomura T. Abdominal visceral fat accumulation is associated with hippocampus volume in non-dementia patients with type 2 diabetes mellitus. NeuroImage 2010;49:57-62.
[20] Jeon BT, Shin HJ, Kim JB. Adiponectin protects hippocampal neurons against kainic acid-induced excitotoxicity. Brain Res Rev 2009;61:81-8.

Peptides 35 (2012) 131–135

Contents lists available at SciVerse ScienceDirect

Peptides

journal homepage: www.elsevier.com/locate/peptides

Short communication

Intracerebroventricular administration of urotensin II regulates food intake and sympathetic nerve activity in brown adipose tissue

Tohru Yasuda, Takayuki Masaki*, Koro Gotoh, Seiichi Chiba, Tetsuya Kakuma, Hironobu Yoshimatsu

Department of Internal Medicine I, Faculty of Medicine, Oita University, 1-1, Idaigaoka, Hasama, Oita 879-5593, Japan

ARTICLE INFO

Article history:
Received 11 January 2012
Received in revised form 1 March 2012
Accepted 1 March 2012
Available online 10 March 2012

ABSTRACT

To clarify the functional roles of urotensin II in regulating energy balance, we investigated the effects of a central infusion of urotensin II on food intake, uncoupling protein (UCP) 1 mRNA expression, temperature, and sympathetic nervous system activity in brown adipose tissue (BAT), a site that regulates energy expenditure in rodents. A bolus central infusion of urotensin II at a dose of 1 nmol/rat into the third cerebral ventricle decreased food intake ($p < 0.05$). Additionally, urotensin II induced c-Fos-like-immunoreactivity (c-FLI) in the paraventricular nucleus (PVN) as compared with that in the control (phosphate buffered saline [PBS]-treated) group. Furthermore, urotensin II increased BAT UCP 1 mRNA expression ($p < 0.05$). Finally, central infusion of urotensin II significantly increased BAT sympathetic nerve activity, which was accompanied by a significant elevation in BAT temperature ($p < 0.05$) in rats. Taken together, central infusion of urotensin II regulates food intake and BAT sympathetic nerve activity in rats.

1. Introduction

Urotensin II is a vasoactive somatostatin-like cyclic peptide that was originally isolated from the fish spinal cord [2,6] and has since been cloned from humans [7]. Research on fish and frog urotensin II has demonstrated the cardiovascular effects of this peptide [11,13,24], which is involved in osmoregulation and the regulation of lipid metabolism [6]. Furthermore, since the urotensin II receptor G-protein coupled receptor 14 (GPR14) is also expressed extensively in glial cells within the brainstem, thalamus, and hypothalamus [14], it may have additional activities.

Uncoupling protein (UCP) is an inner mitochondrial membrane transporter of free fatty acids that dissipates the proton gradient by releasing stored energy as heat [18]. UCP1 in brown adipose tissue (BAT) plays a major role in energy expenditure and thermogenesis in rodents and mammalian species, including humans. BAT UCP1 is regulated by the sympathetic nervous system and several peripheral factors [16,17]. To date, central administration of feeding-related neuropeptides, such as melanin stimulating hormone (MSH) and corticotropin releasing hormone (CRH), have been shown to affect the activity of sympathetic nerves innervating BAT [8,25].

Little is known regarding how an infusion of urotensin II into the third cerebral ventricle (i3vt) affects BAT. To address these issues, the present study clarified the effects of acute central administration of urotensin II on BAT temperature, BAT sympathetic nerve activity, and food intake.

2. Materials and methods

2.1. Animals

Male Sprague-Dawley rats (8–10 weeks old; Seac Yoshitomi, Fukuoka, Japan) were maintained on a 12:12 h light:dark photoperiod (lights on at 0700 h) in a temperature (21 ± 1 °C) and humidity (55 ± 5%) controlled room. We used standard powdered food (CLEA Japan, Tokyo, Japan) ad libitum. Daily food consumption and body weights were measured at 1500 h. Measurements were monitored 4 and 24 h after urotensin II infusion (1900 and 1500 h). All studies were conducted in accordance with Oita Medical University Guidelines, which are based on the *National Institutes of Health Guide for the Care and Use of Laboratory Animals.*

2.2. Reagents

Urotensin II (Sigma, St. Louis, MO) was dissolved in phosphate-buffered saline (PBS) to a concentration of 1×10^{-4} M (adjusted pH 6.4–7.2). Solutions were prepared on the day of administration.

* Corresponding author. Tel.: +81 975 86 5790/5792; fax: +81 975 49 4480.
E-mail address: masaki@oita-u.ac.jp (T. Masaki).

0196-9781/$ – see front matter © 2012 Elsevier Inc. All rights reserved.
doi:10.1016/j.peptides.2012.03.001

2.3. Cerebroventricular cannula implantation

Each rat was fixed in a stereotaxic apparatus (Narishige, Japan) under sodium pentobarbital anesthesia (45 mg/kg, i.p.) and a stainless steel guide cannula (23 gauge) was implanted chronically into the i3vt. A stainless steel wire stylet (29 gauge) was left in the guide cannula to keep it patent and prevent leakage of cerebrospinal fluid. Surgery was carried out at least one week prior to the infusion of the test solutions; the details of the surgical procedure have been described elsewhere [28].

2.4. Measurement of food intake

All rats were handled for 5 min daily on three successive days before each experiment to equilibrate their arousal levels. The rats that underwent surgery were allowed to recover for five days before the experiment. On the day of testing, the rats were confirmed to have had normal food intake and have normal body weight. Eight weight-matched rats were divided into two groups ($n = 4$ for each) and were treated with urotensin II (0, 0.01, 0.1, and 1 nmol). The dose of urotensin II was based on our preliminary and previous studies [12,14,15,23]. Test solutions were administered at 1900 h to unrestrained, unanesthetized rats via an i3vt cannula at a rate of 1.0 μl/min for 10 min. Cumulative food consumption was measured for 4 and 24 h after urotensin II treatment. c-Fos-like immunoreactivity (c-FLI), BAT UCP expression, and sympathetic nerve activity were measured at 0, 1, 1.5, or 2 h after urotensin II treatment.

2.5. c-fos like immunoreactivity

To prevent stress-induced c-fos expression on the test day, rats were regularly handled during recovery from surgery. On the test day, rats were given i3vt infusion of urotensin II (1 nmol) or PBS ($n = 4$ for each). Then, 0, 1, 1.5 and 2 h after injection, rats were anesthetized with Nembutal (3.3 ml/kg, i.p.) and transcardially perfused with isotonic PBS followed by 4% paraformaldehyde in 0.1 M phosphate buffer. Brains were removed and postfixed for 24 h and then processed for c-FLI. Forty-micrometer slices were cut from the brain with a microtome. Forebrain slices were made in the coronal plane to allow visualization of the central nucleus of the various nuclei of the hypothalamus [the PVN, ventromedial nucleus (VMH), arcuate nucleus (ARC), and lateral hypothalamic area (LHA)]. Tissues were rinsed (3× PBS), incubated for 1 h in 0.3% H_2O_2 in absolute methanol to quench endogenous peroxidase, and rinsed (3× PBS). Slices were then transferred without rinsing to the primary antibody solution, consisting of 0.005 g/ml polyclonal rabbit anti-serum (Santa Cruz Biotechnology Inc., Santa Cruz, CA), which recognizes residues 3–16 of the c-Fos protein. After 24 h of incubation on ice, slices were rinsed (3× PBS) and processed with the ABC method (Vector Laboratories, Burlingame, CA). Slices were transferred to biotinylated goat antirabbit antibody for 1 h, rinsed, transferred to avidin-biotinylated peroxidase for 1 h, rinsed, and developed with diaminobenzidine substrate (6 min). Slices were rinsed, mounted on slides, and coverslipped with Permount. Camera lucida drawings of c-Fos-positive brain structures were prepared by an experimenter naive to group treatments. Care was taken so that structures were scored in approximately the same plane. Drawings were scored by blinded raters who recorded the number and location of c-Fos-positive nuclei (Olympus Corp. Optical Co. Ltd., Tokyo, Japan). Scores across raters were averaged for statistical analyses.

2.6. Real-time quantitative RT-PCR

BAT was dissected 1.5 h after urotensin II treatment. BAT UCP1, UCP2 and UCP3 mRNA was amplified by PCR and quantified using real-time quantitative PCR as follows. Total cellular RNA was prepared from BAT tissues using TRIzol (Lifetech, Tokyo, Japan) according to the manufacturer's protocol. Total RNA (20 μg) was electrophoresed on 1.2% formaldehyde agarose gels. RNA quality and quantity were assessed using EtBr agarose gel electrophoresis and by measuring the absorbance at 260 nm relative to that at 280 nm. cDNA was synthesized from total RNA (150 ng) in a volume of 20 μl using a ReverTra-Dash reverse transcriptase kit (Toyobo, Tokyo, Japan) with random hexamer primers. The reactions were diluted to 50 μl with sterile distilled water and stored at −20 °C. Primers were designed, synthesized, optimized, and obtained as preoptimized kits: UCP1 (Catalog No. Mm00494069m1), UCP2 (Catalog No. Mm00495907m1), and UCP3 (Catalog No. Mm00494074m1). Primers for ribosomal RNA for use as an internal control was also obtained as a preoptimized kit (Catalog No. Hs99999901). These preoptimized kits were purchased from Applied Biosystems (Foster City, CA). Using an ABI PRISM 7000 sequence detector (Applied Biosystems), PCR amplification was performed in 50-μl volumes containing 100 ng cDNA template in PCR Master Mix (Roche, Nutley, NJ), according to the following protocol: 50 days for 2 min, 95 °C for 10 min, and 40 cycles at 95 °C for 15 s and 60 °C for 1 min. Samples were analyzed in duplicate. Target mRNA amounts were normalized to ribosomal RNA. In brief, target genes and ribosomal RNA values were calculated from standard curves obtained by amplification of twofold serial dilutions of cDNA from the tissue. We verified that the cDNAs and ribosomal RNA were amplified at approximately the same efficiency. Results are expressed as the percent of ribosomal RNA-normalized target mRNA in experimental groups vs. control groups. The results were analyzed using sequence detection software (Applied Biosystems), as outlined in PerkinElmer's user bulletin no. 2 (PerkinElmer, Wellesley, MA).

2.7. Measurement of BAT temperature

A plastic-coated thermocouple was inserted into the interscapular BAT of rats, each with an i3vt cannula, under anesthesia (urethane, α-chloralose; Sigma, Tokyo, JPN). The temperature was measured at 10-min intervals for 60 min after urotensin II or PBS was infused as described above.

2.8. Measurement of BAT sympathetic nerve activity

After being allowed 7–10 days to recover from surgery, experiments were carried out under anesthesia. After dissection of the fine branches of the intercostal nerves that supply the interscapular BAT, the nerves were transected where they entered the IBAT. Electrical discharges were recorded from fine filaments placed proximal to the transaction site using bipolar tungsten wire electrodes immersed in heavy white mineral oil to prevent dehydration of the nerves. Discharges were amplified through a condenser-coupled differential input preamplifier and fed into a window discriminator to differentiate signals from background noise. The number of pulses was integrated over 5 s. During stable periods of neuronal activity, Urotensin II was infused via a 30-gauge infusion cannula that was lowered to 1 mm below the tip of the guide cannula. Urotensin II was infused into the third ventricle (0 nmol, 0.01 nmol, 0.1 nmol and 1 nmol/10 μl) over 10 min. Controls were infused with PBS alone. The method used to record nerve has been described elsewhere [19,25–27].

2.9. Statistical analysis

Differences among groups were assessed using two-way ANOVA with repeated measures and the Dunnett test for multiple comparisons. A two-sided p value of less than 0.05 was considered

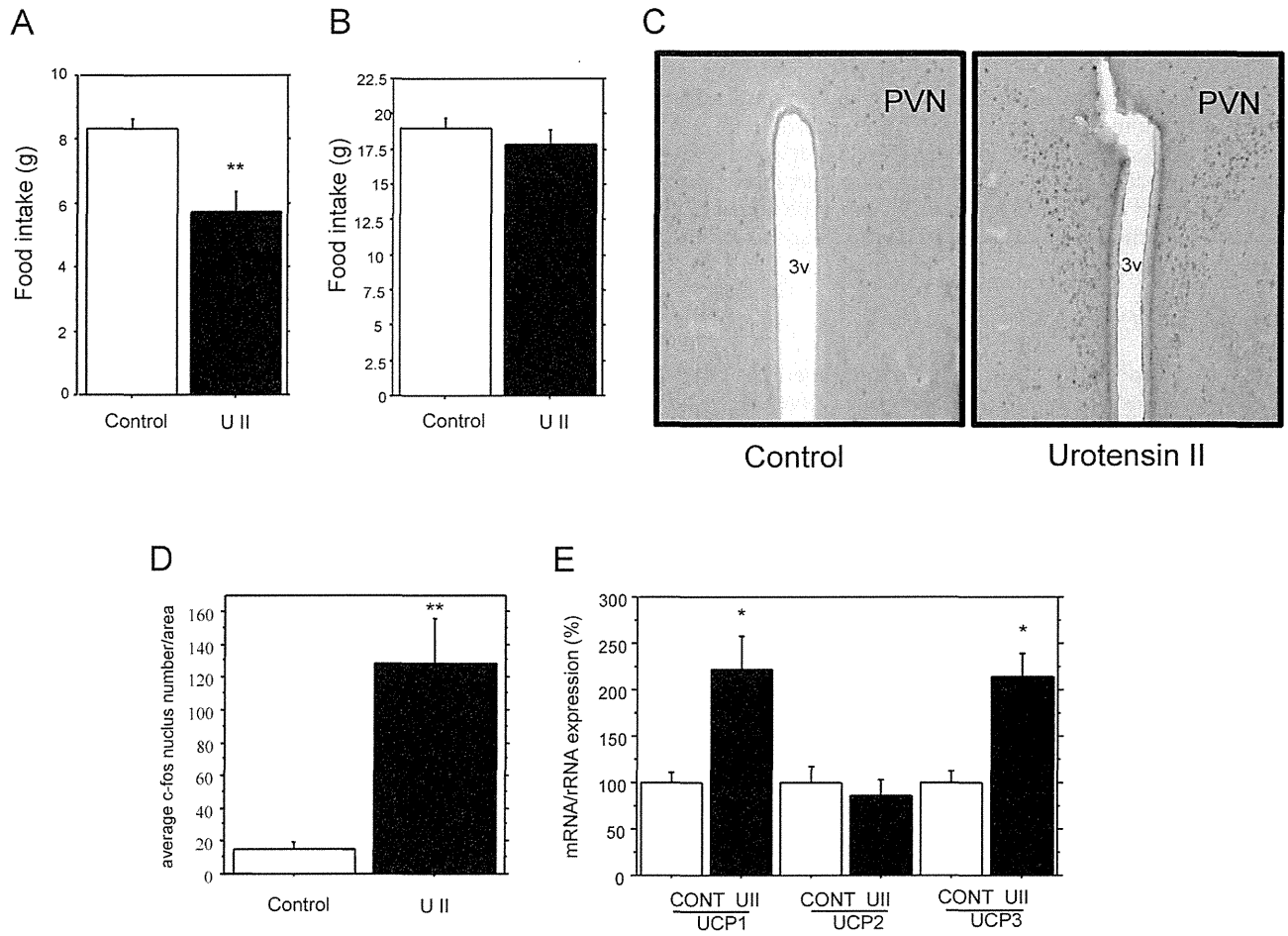

Fig. 1. Effects of intra third cerebroventricular (i3vt) infusion of urotensin II (1 nmol) or phosphate-buffered saline (PBS; control group) on cumulative 4 h (A) and 24 h (B) food intake. Effects of i3vt infusion of urotensin II or PBS on c-fos in the Paraventricular nucleus (PVN). Representative photomicrographs of c-fos (C) and average c-fos number in PVN (D). Effects of i3vt infusion of urotensin II or PBS on BAT uncoupling protein (UCP)1, UCP2 and UCP3 mRNA expression (E). All data are the mean ± SEM ($n = 4$ per group). Uroteinsin II (U II). $^{*}p < 0.05$, $^{**}p < 0.01$ vs. controls.

statistically significant. The dose-dependent effects were assessed by Fishers Z score.

3. Results

Central administration of urotensin II (1 nmol) caused a significant decrease in food intake over 4 h as compared with control animals (controls: 8.3 ± 0.3 g vs. urotensin II: 5.7 ± 0.6 g; Fig. 1A; $p < 0.05$). Food consumption recovered within 24 h after urotensin II treatment (controls: 18.9 ± 0.7 g vs. urotensin II: 17.8 ± 1.1 g; Fig. 1B).

The numbers of c-FLI-positive cells in the paraventricular nucleus (PVN) are shown in Fig. 1C and D, and representative photomicrographs of the PVN are presented in Fig. 1C. Administration of urotensin II to rats caused induction of c-FLI in the PVN after 1.5 h (Fig. 1C and D; $p < 0.05$), but not in the arcuate nucleus, ventromedial nucleus, or lateral hypothalamic area as compared with that in the control group. Results of a time-course study with urotensin II revealed that the best time for c-Fos expression in the PVN was 1.5 h after treatment (0 min, 9 ± 3; 60 min, 85 ± 16; 90 min, 127 ± 26; 120 min, 71 ± 15 per PVN).

Fig. 1E shows the changes in BAT UCP1, UCP2, and UCP3 mRNA levels after urotensin II treatment. BAT UCP1 and UCP3 mRNA expression increased after treatment with urotensin II as compared with that in controls ($p < 0.05$ for each). No significant change occurred in white adipose tissue (WAT) UCP2 mRNA expression in the urotensin II group as compared with the controls.

Ventricular infusion of urotensin II caused a rapid and significant elevation in BAT temperature as compared with controls ($p < 0.05$) (Fig. 2A). In addition, BAT temperature reached a nadir about 50–60 min after the infusion and gradually recovered.

Dose-dependent effects of urotensin II were observed ($R^2 = 0.72$, $p < 0.01$) on sympathetic nerve activity. Fig. 2B illustrates the typical responses of BAT sympathetic nerve activity in response to the ventricular infusion of urotensin II. Sympathetic nerve activity increased significantly after the central administration of urotensin II. This response reached a peak about 20–30 min after the infusion and gradually recovered. Mean changes in sympathetic nerve activity in response to urotensin II treatment were statistically different from those in the control (phosphate buffered saline [PBS]-treated) group ($p < 0.05$ or $p < 0.01$; Fig. 2C).

4. Discussion

We initially investigated the acute effects of centrally administered urotensin II on BAT temperature and BAT sympathetic nerves in urethane anesthetized rats. The results showed that urotensin II treatment increased BAT temperature with a time course similar to that seen for sympathetic nerve activity. It has been reported previously that central administration of urotensin

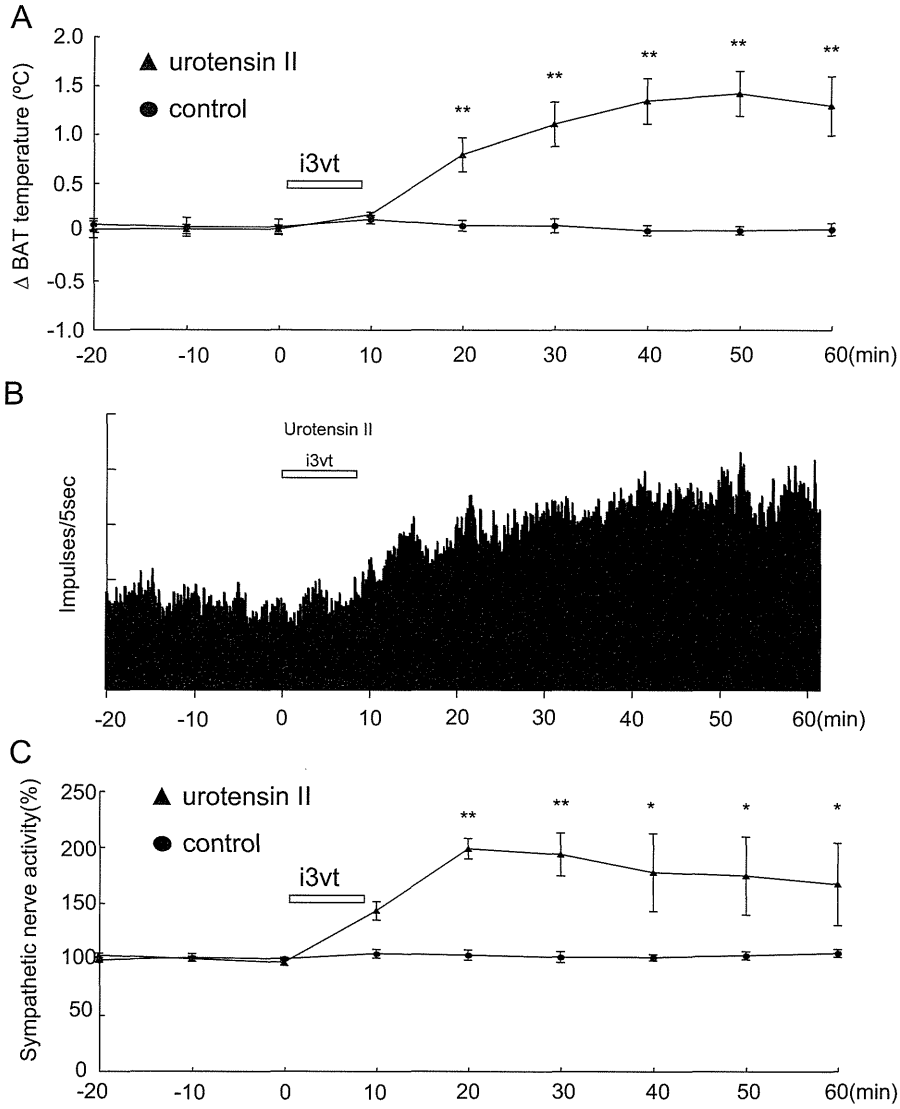

Fig. 2. Effects of i3vt infusion of urotensin II (1 nmol) or PBS (control) on BAT temperatures (A). Rate meter plots of BAT sympathetic nerve activity following i3vt infusion of urotensin II (B). Vertical axis: nerve impulses per 5 s. Bold horizontal bar: urotensin II infusion. Percentage differences in sympathetic nerve activity from baseline (100%) after i3vt infusion of urotensin II or PBS (C). Horizontal bars: 10-min time scale. All data are the mean ± SEM ($n = 4$ per group). ▲ = urotensin II -treated animals. ● = control. $^{*}p < 0.05$, $^{**}p < 0.01$ vs. controls.

II significantly increases rearing and grooming behaviors, and increases motor activity in a familiar environment [10]. Central administration of urotensin II produces presser and tachycardiac responses through sympathetic activation [15]. Administration of a β_3 agonist increases UCP1 mRNA expression in BAT [29]. In the present study, urotensin II increased sympathetic nerve activity and BAT UCP1 and UCP3 mRNA expression. Based on previous studies, human urotensin II is known to increase plasma prolactin and thyroid stimulating hormone levels [10] and chronic treatment with thyroid hormone increases UCP1 mRNA expression in BAT [17]. It is therefore possible that thyroid hormone might have modulated BAT sympathetic nerve activity in the present study.

Sympathetic nerve activity and food intake are reciprocally related in a number of experimental settings [3,4], including hypothalamic lesions, peptide injection, or treatment with several drugs. MSH decreases food intake when injected into the third cerebroventricle and increases BAT sympathetic nerve activity [25]. In addition, injection of CRH into the third cerebroventricle decreases food intake and increases BAT sympathetic nerve activity [1,8]. In the present study, urotensin II decreased food intake and increased BAT sympathetic nerve activity. These results are consistent with previous studies suggesting that increased food intake is usually associated with low levels of sympathetic activity and vice versa [3,4]. Additionally, these responses were accompanied by corresponding changes in BAT temperature, another parameter of UCP1 function. Collectively, our results indicate that urotensin II may regulate energy expenditure and thermogenesis during the acute phase through efferent sympathetic nerves.

A great deal of interest has been focused on the urotensin II system in relation to health and disease [21]. Previous studies have suggested a relationship between urotensin II and metabolic syndrome, including obesity, hypertension, insulin resistance, hyperglycemia, and lipid metabolism. Indeed, some reports suggest that urotensin II is a marker for disease activity [9,20]. Urotensin II is associated with insulin resistance and type 2 diabetes. Increases in adipose tissue elevate free fatty acid levels in the plasma via both the hydrolysis of triglycerides and the lipolysis of lipoproteins. Lipolytic enzyme activity within adipose tissue is significantly enhanced by urotensin II treatment [22]. In addition to systolic and diastolic blood pressure, plasma urotensin II levels are correlated

with body weight [5]. Our results demonstrated that central administration of urotensin II regulates not only food intake but also BAT UCP mRNA expression and sympathetic nerve activity. Taken together, these studies indicate that the urotensin II system is also involved in obesity and may be a target for therapeutic intervention for metabolic syndrome.

Conflict of interest

Nothing to disclose.

Acknowledgments

This work was supported by Grants-in-Aid from the Japanese Ministry of Education, Science and Culture, by Research Grants for Intractable Diseases from the Japanese Ministry of Health and Welfare.

References

[1] Arase K. Effects of corticotropin-releasing factor on food intake and brown adipose tissue thermogenesis in rats. Am J Physiol 1988;255:E255–9.
[2] Bern HA, Pearson D, Larson BA, Nishioka RS. Neurohormones from fish tails: the caudal neurosecretory system. I. Urophysiology and the caudal neurosecretory system of fishes. Recent Prog Horm Res 1985;41:533–52.
[3] Bray GA. Reciprocal relation between the sympathetic nervous system and food intake. Brain Res Bull 1991;27:517–20.
[4] Bray GA. Peptides affect the intake of specific nutrients and the sympathetic nervous system. Am J Clin Nutr 1992;55:265S–71S.
[5] Cheung BM, Leung R, Man YB, Wong LY. Plasma concentration of urotensin II is raised in hypertension. J Hypertens 2004;22:1341–4.
[6] Conlon JM, Yano K, Waugh D, Hazon N. Distribution and molecular forms of urotensin II and its role in cardiovascular regulation in vertebrates. J Exp Zool 1996;275:226–38.
[7] Coulouarn Y, Lihrmann I, Jegou S, Anouar Y, Tostivint H, Beauvillain JC, et al. Cloning of the cDNA encoding the urotensin II precursor in frog and human reveals intense expression of the urotensin II gene in motoneurons of the spinal cord. Proc Natl Acad Sci U S A 1998;95:15803–8.
[8] Egawa M. Preoptic area injection of corticotropin-releasing hormone stimulates sympathetic activity. Am J Physiol 1990;259:R799–806.
[9] Eckel RH, Grundy SM, Zimmet PZ. The metabolic syndrome. Lancet 2005;365:1415–28.
[10] Gartlon J, Parker F, Harrison DC, Douglas SA, Ashmeade TE, Riley GJ, et al. Central effects of urotensin-II following ICV administration in rats. Psychopharmacology (Berlin) 2001;155:426–33.
[11] Gibson A, Conyers S, Bern HA. The influence of urotensin II on calcium flux in rat aorta. J Pharm Pharmacol 1988;40:893–5.
[12] Hood SG, Watson AM, May CN. Cardiac actions of central but not peripheral urotensin II are prevented by beta-adrenoceptor blockade. Peptides 2005;26:1248–56.
[13] Itoh H, Itoh Y, Rivier J, Lederis K. Contraction of major artery segments of rat by fish neuropeptide urotensin II. Am J Physiol 1987;252:R361–6.
[14] Lin Y, Tsuchihashi T, Matsumura K, Fukuhara M, Ohya Y, Fujii K, et al. Central cardiovascular action of urotensin II in spontaneously hypertensive rats. Hypertens Res 2003;26:839–45.
[15] Lin Y, Tsuchihashi T, Matsumura K, Abe I, Iida M. Central cardiovascular action of urotensin II in conscious rats. J Hypertens 2003;21:159–65.
[16] Masaki T, Yoshimatsu H, Kakuma T, Chiba S, Hidaka S, Tajima D, et al. Induction of rat uncoupling protein-2 gene treated with tumour necrosis factor alpha in vivo. Eur J Clin Invest 1999;29:76–82.
[17] Masaki T, Yoshimatsu H, Sakata T. Expression of rat uncoupling protein family mRNA levels by chronic treatment with thyroid hormone. Int J Obes Relat Metab Disord 2000;24:S162–4.
[18] Nicholls DG, Locke RM. Thermogenic mechanisms in brown fat. Physiol Rev 1984;64:1–64.
[19] Niijima A. Nervous regulation of metabolism. Prog Neurobiol 1989;33:135–47.
[20] Ong KL, Wong LY, Cheung BM. The role of urotensin II in the metabolic syndrome. Peptides 2008;29:859–67.
[21] Ross B, McKendy K, Giaid A. Role of urotensin II in health and disease. Am J Physiol Regul Integr Comp Physiol 2010;298:R1156–72.
[22] Sheridan MA, Plisetskaya EM, Bern HA, Gorbman A. Effects of somatostatin-25 and urotensin II on lipid and carbohydrate metabolism of coho salmon, *Oncorhynchus kisutch*. Gen Comp Endocrinol 1987;66:405–14.
[23] Watson AM, Lambert GW, Smith KJ, May CN. Urotensin II acts centrally to increase epinephrine and ACTH release and causes potent inotropic and chronotropic actions. Hypertension 2003;42:373–9.
[24] Yano K, Hicks JW, Vaudry H, Conlon JM. Cardiovascular actions of frog urotensin II in the frog, Rana catesbeiana. Gen Comp Endocrinol 1995;97:103–10.
[25] Yasuda T, Masaki T, Kakuma T, Yoshimatsu. H Hypothalamic melanocortin system regulates sympathetic nerve activity in brown adipose tissue. Exp Biol Med (Maywood) 2004;229:235–9.
[26] Yasuda T, Masaki T, Sakata T, Yoshimatsu H. Hypothalamic neuronal histamine regulates sympathetic nerve activity and expression of uncoupling protein 1 mRNA in brown adipose tissue in rats. Neuroscience 2004;125:535–40.
[27] Yasuda T, Masaki T, Chiba S, Kakuma T, Sakata T, Yoshimatsu H. L-histidine stimulates sympathetic nerve activity to brown adipose tissue in rats. Neurosci Lett 2004;362:71–4.
[28] Yoshimatsu H, Egawa M, Bray GA. Sympathetic nerve activity after discrete hypothalamic injection of L-glutamate. Brain Res 1993;601:121–8.
[29] Yoshitomi H, Yamazaki K, Abe S, Tanaka I. Differential regulation of mouse uncoupling proteins among brown adipose tissue, white adipose tissue, and skeletal muscle in chronic beta 3 adrenergic receptor agonist treatment. Biochem Biophys Res Commun 1998;253:85–91.

METABOLISM CLINICAL AND EXPERIMENTAL 61 (2012) 1312–1320

Available online at www.sciencedirect.com

Metabolism

www.metabolismjournal.com

Intestinal fatty acid infusion modulates food preference as well as calorie intake *via* the vagal nerve and midbrain–hypothalamic neural pathways in rats

Nobuya Ogawa[a,c], *Makoto Ito*[b,c], *Hideki Yamaguchi*[a], *Tetsuya Shiuchi*[b], *Shiki Okamoto*[b], *Korekiyo Wakitani*[c], *Yasuhiko Minokoshi*[b], *Masamitsu Nakazato*[a,*]

[a] *Division of Neurology, Respirology, Endocrinology and Metabolism, Department of Internal Medicine, Faculty of Medicine, University of Miyazaki, 5200 Kihara, Kiyotake, Miyazaki 889-1692, Japan*

[b] *Division of Endocrinology and Metabolism, Department of Developmental Physiology, National Institute for Physiological Sciences, 38 Nishigonaka, Myodaiji, Okazaki 444-8585, Japan*

[c] *Biological/Pharmacological Research Laboratories, Central Pharmaceutical Research Institute, JT Inc., 1-1 Murasaki-cho, Takatsuki 569-1125, Japan*

ARTICLE INFO

Article history:
Received 2 December 2011
Accepted 23 February 2012

ABSTRACT

The intestine plays important roles in the regulation of feeding behavior by sensing macronutrients. Intestinal fatty acids strongly suppress food intake, but little is known about whether intestinal fatty acids affect food preference. We investigated the effects of jejunal fatty acids infusion on food preference by conducting two-diet choice experiments in rats fed a high-fat diet (HFD) and a high-carbohydrate diet (HCD). Jejunal linoleic acid (18:2) infusion reduced HFD intake dose-dependently, while HCD intake increased with the middle dose of the infusion we examined (100 μL/h) and reduced to the control level with the higher doses (150 and 200 μL/h). α-Linolenic acid (18:3), but not caprylic acid (8:0), altered the food preference and total calorie intake in the same manner as linoleic acid. Linoleic acid infusion dose-dependently increased plasma glucagon-like peptide-1, peptide YY and cholecystokinin levels, but not ghrelin levels. Subdiaphragmatic vagotomy or midbrain transection prevented the change in food preference and total calorie intake by linoleic acid infusion. Jejunal linoleic acid infusion increased norepinephrine turnover in the paraventricular hypothalamic nucleus, while intracerebroventricular injection of idazoxan, an α2-adrenergic receptor (AR) antagonist, suppressed the increased HCD intake, but did not affect the decreased HFD intake. These findings indicated that intestinal long-chain fatty acids modulated food preference as well as total calorie intake *via* the vagal nerve and midbrain–hypothalamic neural pathways. The effects of the α2-AR antagonist in the brain suggested that the brain distinctly controlled HCD and HFD intake in response to jejunal linoleic acid infusion.

Abbreviations: AR, adrenergic receptor; ARC, arcuate nucleus; CCK, cholecystokinin; DA, dopamine; DMH, dorsomedial hypothalamus; GLP-1, glucagon-like peptide-1; HCD, high-carbohydrate diet; HFD, high-fat diet; LH, lateral hypothalamus; α-MT, α-methyl-*p*-tyrosine; NAc, nucleus accumbens; NE, norepinephrine; NTS, nucleus of the solitary tract; PVH, paraventricular hypothalamic nuclei; PYY, peptide YY; VMH, ventromedial hypothalamus.

* *Corresponding author.* Tel.: +81 985 85 2965; fax: +81 985 85 1869.
E-mail address: nakazato@med.miyazaki-u.ac.jp (M. Nakazato).

0026-0495/$ – see front matter © 2012 Elsevier Inc. All rights reserved.
doi:10.1016/j.metabol.2012.02.011

1. Introduction

Humans as well as rodents show a strong preference for fat diets [1–4]. Obese subjects show a greater preference for fatty foods than non-obese subjects [3,4]. Correcting the preference for food stuffs is a beneficial treatment for obese or type 2 diabetes mellitus patients [5]. The intestine has important roles in the regulation of energy homeostasis as well as the principal roles in the digestion and absorption of nutrients. It has been postulated that the intestine has specific cells that express receptors for nutrient perception and transmit signals to the brain [6–11]. Long-chain fatty acids potently suppress food intake, compared with short- or medium-chain fatty acids [12]. Intestinal fatty acids stimulate the release of anorectic gut hormones [13–15] and increase the levels of fatty acid derivative [16,17], subsequently transmitting the visceral sensory information to the hypothalamus and brain stem *via* the vagal afferent nerve and/or through the bloodstream [17–20]. The suppression of food intake in response to intestinal fatty acids is partially reversed by vagal denervation [21]. Short-term infusion of oleic acid increases the levels of intestinal oleylethanolamide thereby decreasing food intake through the activation of nuclear receptor PPAR-α and vagal afferent nerves [16,17]. However, the effect of fatty acid infusion on food preference remains elusive. To determine the regulatory role of intestinal fatty acids in food preference, we conducted food-choice experiments in rats with jejunal fatty acid infusion. The rats were given a free choice of a high-fat diet (HFD) and a high-carbohydrate diet (HCD), because fats and carbohydrates are the main sources of food energy. We found that jejunal infusion of long-chain fatty acids, including linoleic acid, preferentially suppressed HFD intake but not HCD intake. HCD intake was rather increased with the middle dose of linoleic acid (100 μL/h), and then decreased to the control level with the higher infusion doses (≥150 μL/h).

Visceral sensory information is transmitted to the nucleus of the solitary tract (NTS) *via* the vagal afferent nerves [22]. The signals are then relayed to not only the hypothalamus but also the mesolimbic "reward" circuits through the dorsal and ventral bundles of catecholaminergic neurons, which include dopamine (DA) neurons originating from the ventral tegmental area and reaching the nucleus accumbens (NAc) [23]. It has been shown that norepinephrine (NE) injection into the paraventricular hypothalamic nucleus (PVH) preferentially stimulates carbohydrate feeding through the α2-adrenergic receptor (AR) [24,25]. Orosensory stimuli derived with corn oil or high-fat feeding also increase DA release in the NAc [26,27]. Therefore, assuming that neuronal pathways and brain areas are involved in the change in food preference after jejunal fatty acid infusion, we investigated the effects of vagotomy and midbrain transaction, the NE and DA turnovers in these brain areas, and the effects of a specific α2-AR antagonist in the brain. Jejunal linoleic acid infusion modulated food preference through the vagal nerve and midbrain–hypothalamic neural pathways and NE system in the PVH.

2. Materials and methods

2.1. Animals

Male Sprague–Dawley rats (Charles River Japan, Shiga, Japan) weighing 280–320 g at surgery were housed individually in cages under controlled temperature (22–24 °C) and light (lights on 22:00–10:00) conditions. The rats were given access to both an HFD and an HCD. Macronutrient sources and compositions were indicated in Table 1. Energy contents of the diets were 5.1 kcal/g for the HFD and 3.3 kcal/g for the HCD, respectively. All procedures were conducted in accordance with the Japanese Physiological Society guidelines for animal care.

2.2. Intrajejunal cannulation

Prior to surgery, the rats were fasted overnight and then anesthetized with intraperitoneal 50 mg/kg pentobarbital sodium (Abbott Laboratories, Chicago, IL). After abdominal celiotomy, a polyethylene tube (SP28; I.D. 0.4 mm, O.D. 0.8; mm, Natsume, Tokyo, Japan) was inserted into the duodenum (5 cm from the pylorus). The end of the tube reached the proximal jejunum (10 cm from the pylorus). The tube was fixed to the entrance of the intestine with silk sutures. The opposite end of the tube was threaded through the opening in the abdominal wall and tunneled subcutaneously to the dorsal surface of the neck, where a Dacron mesh anchor button (DC95; Instech Solomon, Plymouth Meeting, PA) was implanted. The tube was also fixed to the ventral abdominal wall and the anchor button mesh using silk sutures. The rats were allowed to recover for 1–2 weeks and become sufficiently adapted to the continuous infusion apparatus (Instech Solomon) before further experiments were performed. Daily food intakes of both diets were monitored continuously to assess the recovery after surgery and adaptation to the apparatus.

2.3. Feeding tests

At 1 h before onset of the dark phase, both diets were removed from the cage. Linoleic acid (Nacalai Tesque, Tokyo, Japan), α-linolenic acid (Nacalai Tesque), caprylic acid (Nacalai Tesque) or saline was then infused into the jejunum at rates of 50, 100, 150 or 200 μL/h. At the onset of the dark phase, 1 h after starting the infusion, the HFD and HCD were provided again. The jejunal infusion of linoleic acid continued for 7 h (−1 to 6 h) and the cumulative food intake was measured at 3, 6 and 23 h,

Table 1 – Macronutrient sources and compositions of HFD and HCD.

Macronutrient	Source	HFD		HCD	
		wt %	cal %	wt %	cal %
Carbohydrate	Starch	7.3	5.0	39.2	41.7
	Sucrose	14.4	10.7	14.4	16.8
Fat	Lard	35.0	63.4	3.1	8.8
Protein	Casein	28.8	20.9	28.8	32.7

while the other infusions lasted for 4 h (–1 to 3 h) and the food intake was measured at 3 h, except for the measurements of plasma gut hormones in the portal vein (see below). Calorie intake was determined under the following provisions: fat, 9 kcal/g; carbohydrate, 4 kcal/g; protein, 4 kcal/g; fatty acids, 9 kcal/g; weight/volume ratio of fatty acids, 0.9 g/mL. All experiments were conducted in a crossover manner with 3 to 4 days interval, in which all animals received jejunal infusion of fatty acids or saline on separate days. To validate the recovery from each treatment, daily food intakes of both diets were monitored continuously and we confirmed recovery of food intake to pre-treatment level.

2.4. *Measurement of plasma gut hormone levels*

At 1 h before onset of the dark phase, both diets were removed from the cage. Linoleic acid (100 or 200 μL/h) or saline was then infused into the jejunum. The rats were anesthetized with pentobarbital sodium and blood samples were collected from the portal vein after 1 h of infusion. The portal blood samples (2 mL) were mixed with 60 μmol/L EDTA (Wako, Osaka, Japan), 2000 kIU aprotinin (Wako) and 50 μmol/L dipeptidyl peptidase IV inhibitor (Millipore, Billerica, MA). Plasma was separated by centrifugation at 12,000 rpm for 15 min at 4 °C. Plasma glucagon-like peptide-1 (GLP-1) levels were measured using a Glucagon-Like Peptide-1 (Active) ELISA Kit (Millipore), which measures the biologically active forms of GLP-$1_{7\text{-}36}$ and GLP-$1_{7\text{-}37}$ NH2 and does not cross-react with glucagon, GLP-2 or inactive GLP-$1_{9\text{-}37}$ and GLP-$1_{9\text{-}37}$ NH2. Plasma peptide YY (PYY) levels were measured with a Peptide YY EIA Kit (Peninsula Laboratories, San Carlos, CA, USA), which measures the forms of $PYY_{1\text{-}36}$ and $PYY_{3\text{-}36}$ and does not cross-react with NPY. Plasma cholecystokinin (CCK) levels were measured using an EIA for Cholecystokinin Octapeptide (Desulfated) Kit (Peninsula Laboratories), which is specific for CCK-8 (Desulfated) and CCK-33 (sulfated). Plasma ghrelin levels were measured using an Active and Desacyl Ghrelin ELISA Kit (Mitsubishi Chemical Medience, Tokyo, Japan), which measures the biologically active forms of octanoylated $ghrelin_{1\text{-}28}$.

2.5. *Subdiaphragmatic bilateral vagotomy*

Subdiaphragmatic bilateral vagotomy was performed as previously described [18] prior to intrajejunal cannulation. After exposure of the bilateral subdiaphragmatic trunks of the vagus nerve along the esophagus, trunk sections of at least 0.5 cm in length were excised. The rats were allowed to recover for 1–2 weeks and daily food intakes of both diets were monitored continuously to assess the recovery after surgery. To validate the vagotomy, we confirmed that intraperitoneal administration of CCK did not induce an anorectic effect in vagotomized rats [18,28].

2.6. *Bilateral midbrain transection*

Bilateral midbrain transection was performed as previously described [29] prior to intrajejunal cannulation. The heads were fixed in a stereotaxic instrument in a 2.4-mm nose-down position. A 1.5-mm-wide razor was inserted into the brain bilaterally in a coronal plane, 1 mm anterior to the lambdoidal suture, 0.5 mm from the midline and 7.7 mm ventral to the dura. The rats were allowed to recover for 1–2 weeks and daily food intakes of both diets were monitored continuously to assess the recovery after surgery. To validate the efficacy of the midbrain transection surgery, we confirmed that the procedure abrogated the anorectic effect induced by intraperitoneal administration of CCK in transectioned rats [29]. The brains were removed after feeding tests and the location of each lesion was verified histologically. The sectioned noradrenergic fibers were identified by immunostaining with an anti-DA β hydroxylase antiserum (1:1000; Chemicon International, Temecula, CA) using an avidin–biotin complex method [30].

2.7. *Measurements of NE and DA turnover*

NE and DA turnovers were assessed based on decreases in the tissue monoamine concentrations after inhibition of catecholamine biosynthesis with α-methyl-*p*-tyrosine (α-MT) (Sigma, St. Louis, MO) as previously described [31]. At 1 h before onset of the dark phase, both diets were removed from the cage. Linoleic acid or saline infusion into the jejunum was then initiated at a rate of 100 μL/h. At the onset of the dark phase, the rats were injected with α-MT (300 mg/kg, ip). At 0 and 3 h after the α-MT injection, the rats were decapitated and the brain tissues were rapidly removed and weighed. The hypothalamus, cortex, NTS, NAc, striatum and amygdala were dissected from 1-mm-thick coronal sections of fresh brain. The NAc and striatum were dissected from the second sections anterior to the bregma. The amygdala, hypothalamus and cortex were dissected from the third sections caudal to the bregma. The NTS was dissected from the eighth sections caudal to the bregma. The hypothalamic regions were dissected from 1-mm-thick sagittal sections of fresh brain. The arcuate nucleus (ARC), PVH and ventromedial/dorsomedial hypothalamus (VMH/DMH) were dissected from the first sections from the midline of the brain. The lateral hypothalamus (LH) was dissected from the next lateral sections. The coordinates for each brain tissue were as previously described [32,33]. The tissue samples were homogenized in 0.2 mol/L perchloric acid containing 0.1 mmol/L EDTA, and the homogenates were centrifuged at 4 °C. The monoamine contents of the supernatants were assayed by HPLC (EP-300 system; Eicom, Kyoto, Japan) with a reversed-phase column (CA-5ODS; Eicom) and an electrochemical detector (ECD-300; Eicom).

2.8. *Cerebral cannulation*

An intracerebroventricular (icv) cannula was implanted into the third ventricle as previously described [34] prior to intrajejunal cannulation. The heads were fixed in a stereotaxic instrument in a nose-down position. Guide cannulas (22G; Plastic One, Dusseldorf, Germany) were implanted into the third ventricle, 1.8 mm posterior to the bregma, on the midline and 8.6 mm ventral to the dura. To validate the correct location of each cannula, we confirmed that icv administration of angiotensin II induced water drinking. The brains were removed after feeding tests and the location of each cannula was verified histologically.

2.9. *Icv injection of idazoxan*

Idazoxan HCl (Sigma) was dissolved in saline and injected into the third ventricle using an internal cannula (28G; Plastic One) attached to a Hamilton microsyringe. Saline or 25 nmol of idazoxan in a volume of 5 μL was injected over a period of 1 min with the internal cannula left in place for an additional 30 s to permit drug diffusion. Icv injections were performed at 1 h before the onset of the dark phase, just before jejunal linoleic acid infusion.

2.10. *Statistical analysis*

All data are expressed as means ± SEM. Differences between two groups were analyzed using the F-test, followed by Student's *t* test for equal variances or Welch's test for unequal variances. For the multiple comparisons, differences vs saline group were tested using Bartlett's homogeneity of variance test, followed by Dunnett's test for equal variances or Steel's test for unequal variances.

3. Results

3.1. *Jejunal long-chain fatty acid infusion modulates food preference as well as total calorie intake*

Linoleic acid was infused into the jejunum of rats at 50–200 μL/h for 7 h (−1 to 6 h). At 1 h after starting the infusion, the HFD and HCD were provided and the cumulative intake of each diet was measured at 3, 6 and 23 h. Jejunal infusion of linoleic acid dose-dependently decreased HFD intake at all time points, with significant decreases observed at the infusion rates of 100–200 μL/h (Fig. 1A). Differing from the decrease in HFD intake, jejunal linoleic acid infusion did not suppress HCD intake compared with the saline group. HCD intake was significantly increased at the infusion rate of 100 μL/h at 3 h ($P<0.05$) and tended to increase at 6 h (Fig. 1B). HCD intake decreased to the control level with the higher infusion doses (150 and 200 μL/h). As a result, the total calorie intake, including the calories of the infused linoleic acid, was

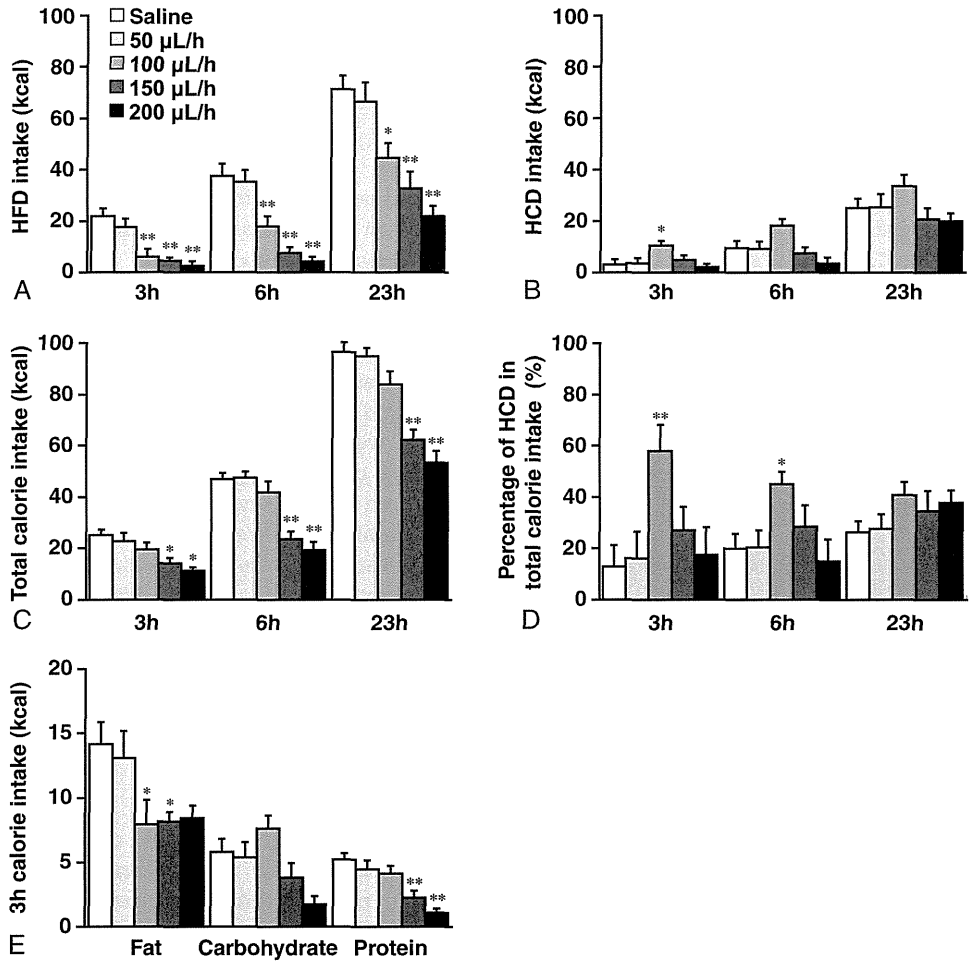

Fig. 1 – Jejunal linoleic acid infusion modulates food preference in rats. Linoleic acid (50–200 μL/h) or saline was infused into the jejunum from −1 to 6 h in rats implanted with a jejunal cannula. The cumulative HFD intake (A) and HCD intake (B) were determined at 3, 6 and 23 h. The total calorie intake, including the calories of the infused linoleic acid infused, was calculated (C). The percentages of HCD in the total calorie intake (D) and macronutrient calorie intake at 3 h (E) were also calculated. The results are expressed as the means ± SEM of seven rats per group. *$P<0.05$ and **$P<0.01$ vs saline infusion by Dunnett's test.

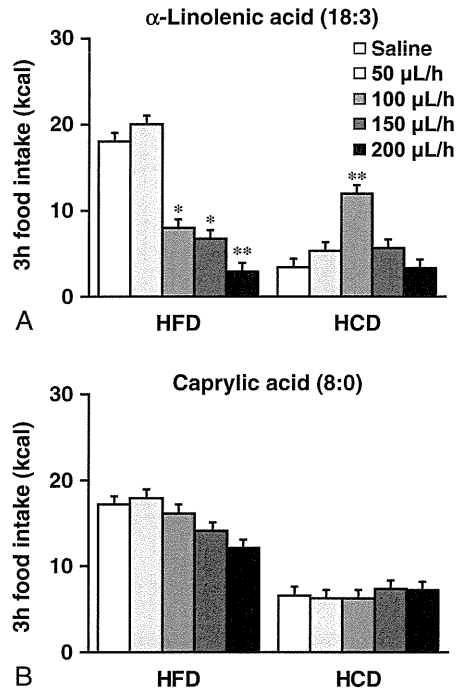

Fig. 2 – Fatty acid chain length affects the induction of food preference modulation. α-Linolenic acid (A) and caprylic acid (B) were infused into the jejunum from −1 to 3 h at rates of 50–200 μL/h. The HFD and HCD intakes were determined at 3 h. The results are expressed as the means ± SEM of eight rats per group. *P < 0.05 and **P < 0.01 vs saline infusion by Dunnett's test.

suppressed at the infusion rates of 150 and 200 μL/h, but not at the infusion rates of 50 and 100 μL/h (Fig. 1C). The percentage of HCD intake in the total calorie intake was significantly increased for the infusion rate of 100 μL/h at 3 and 6 h (Fig. 1D). Concerning the intake of each macronutrient over the first 3 h (Fig. 1E), fat intake, including the calories of the infused linoleic acid, was significantly reduced at the infusion rates of 100 and 150 μL/h, while carbohydrate intake tended to increase at 100 μL/h and to decrease at 200 μL/h. Protein intake was decreased at the infusion rates of 150 and 200 μL/h compared with the saline group. These findings suggest that jejunal linoleic acid infusion decreased HFD intake dose-dependently, while HCD intake did not alter, but rather increased with the middle infusion dose (100 μL/h). Jejunal linoleic acid infusion decreased the total calorie intake only at the higher infusion doses (150 and 200 μL/h).

Next, we examined the effects of α-linolenic acid (18:3), another long-chain fatty acid, and caprylic acid (8:0), a medium-chain fatty acid. α-Linolenic acid infusion had similar effects on the HFD and HCD intakes to linoleic acid (18:2) infusion (Fig. 2A). α-Linolenic acid infusion suppressed HFD intake dose-dependently, while it increased HCD intake at 100 μL/h and decreased HCD intake at 150 and 200 μL/h. Caprylic acid infusion had weaker inhibitory effects on HFD intake than infusion of the long-chain fatty acids, and had no effect on HCD intake (Fig. 2B). Caprylic acid infusion did not affect on HFD and HCD intake at 6 and 23 h (data not shown).

The total calorie intake, including the calories of the infused fatty acids, decreased with α-linolenic acid infusion, but not with caprylic acid infusion.

3.2. *Changes in the plasma level of gut hormones in response to jejunal linoleic acid infusion*

Gut hormones play important roles in food intake regulation. We measured the plasma GLP-1, PYY, CCK and ghrelin levels in portal blood obtained after infusing saline or linoleic acid for 1 h (Fig. 3). Fatty acid infusion increased the plasma GLP-1 and PYY levels dose-dependently at the infusion rates of 100 and 200 μL/h (Fig. 3A and B). The plasma CCK level was slightly increased by fatty acid infusion at 200 μL/h (Fig. 3C), whereas the plasma active ghrelin level was not affected (Fig. 3D). We also evaluated the plasma inactive desacyl ghrelin levels, and confirmed that there was no difference between groups (saline; 4.05 ± 0.64 ng/mL, linoleic acid 100 μL/h; 3.71 ± 0.68 ng/mL, linoleic acid 200 μL/h; 3.83 ± 0.74 ng/mL).

3.3. *Involvement of the neural pathways in the modulation of HCD and HFD intake by jejunal linoleic acid infusion*

To investigate the role of the neural pathway between the intestine and the brain in food preference, we examined the effects of bilateral subdiaphragmatic vagotomy and bilateral

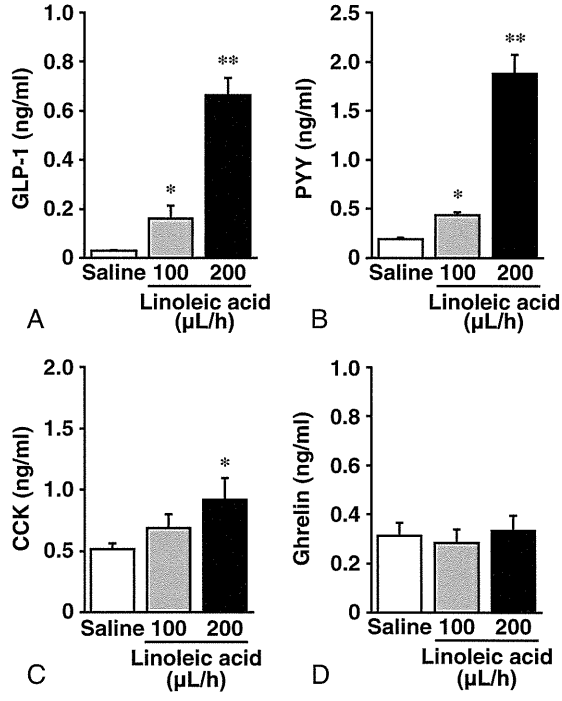

Fig. 3 – Effects of jejunal linoleic acid infusion on plasma gut hormone levels. Linoleic acid (100 or 200 μL/h) or saline was infused into the jejunum for 1 h. Blood samples were collected from the portal vein and the plasma GLP-1 (A), PYY (B), CCK-8 (C) and ghrelin (D) levels were measured. The results are expressed as the means ± SEM of five rats per group. *P < 0.05 and **P < 0.01 vs saline infusion by Dunnett's or Steel's test.

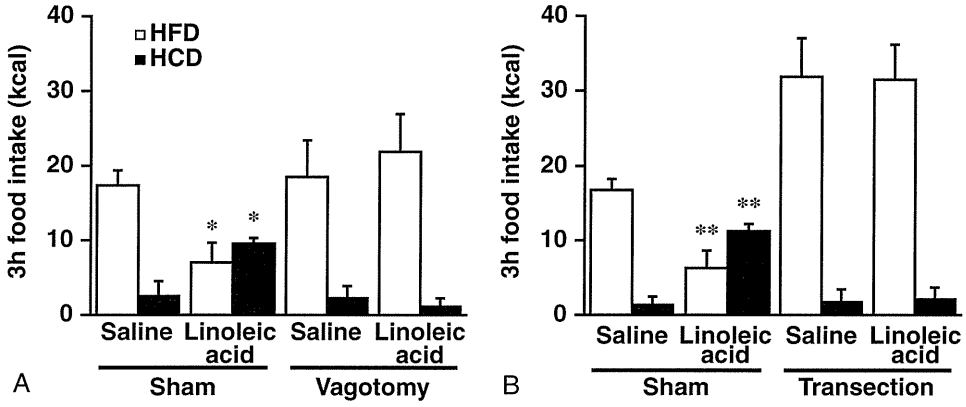

Fig. 4 – Neuronal pathways are involved in the food preference modulation induced by jejunal linoleic acid infusion. Linoleic acid (100 μL/h) or saline was infused into the jejunum from −1 to 3 h in rats that had undergone bilateral subdiaphragmatic vagotomy (A) or bilateral midbrain transection (B). The HFD and HCD intakes were determined at 3 h. The results are expressed as the means±SEM of six rats per group. *P<0.05 vs saline infusion by Student's t test.

midbrain transection on the changes in the HCD and HFD intakes in response to jejunal linoleic acid infusion in rats (Fig. 4). In these experiments, linoleic acid was infused at 100 μL/h, because this rate induced marked changes in food preference, with an increase in HCD intake as well as a decrease in HFD intake. Bilateral subdiaphragmatic vagotomy and bilateral midbrain transection prevented the effects of fatty acid infusion on food preference at 3 h (Fig. 4A and 4B). The similar results were observed at 6 and 23 h between all surgical groups (data not shown). To validate the efficacy of surgeries, we confirmed that intraperitoneal administration of CCK did not induce an anorectic effect in both vagotomized rats (1 h food intake: sham-vehicle; 26.6 ±7.6 kcal, sham-CCK; 12.7±9.0 kcal, $P<0.01$ vs sham-vehicle, vagotomy-vehicle; 19.2±5.9 kcal, vagotomy-CCK; 19.4 ±7.6 kcal) and transectioned rats (1 h food intake: sham-vehicle; 26.5±8.5 kcal, sham-CCK; 12.3±5.6 kcal, $P<0.01$ vs sham-vehicle, transection-vehicle; 28.7±8.6 kcal, transection-CCK; 26.8±8.5 kcal) as described previously [18,28,29]. The brains were removed from transectioned rats after feeding tests and the location of each lesion was verified histologically. The sectioned noradrenergic fibers were identified by immunostaining with an anti-DA β hydroxylase antiserum (data not shown).

3.4. *Intestinal linoleic acid infusion increases NE turnover in the PVH*

The NE and DA turnovers in the brain were measured by assessing the decreases in tissue monoamine contents from the basal levels after inhibition of catecholamine synthesis by an α-MT injection. NE turnover was increased in the PVH, but not in the ARC, LH or VMH/DMH following fatty acid infusion (Fig. 5A), while the basal NE content in the PVH did not differ between the saline and linoleic acid infusion (104.93±9.52 and 111.32±7.74 ng/mg protein, respectively). NE turnover was not affected in the cerebral cortex, NTS, NAc, striatum or amygdala (data not shown). Jejunal linoleic acid infusion did not affect DA turnover in the NAc, striatum, amygdala, hypothalamus, cerebral cortex or NTS (Fig. 5B).

3.5. *An α2-AR antagonist, idazoxan, suppresses the increase in HCD intake induced by jejunal linoleic acid infusion*

NE injection into the PVH stimulates carbohydrate intake preferentially *via* α2-AR signaling [24,25]. We examined whether an α2-AR selective antagonist altered the increase in HCD intake and decrease in HFD intake in response to

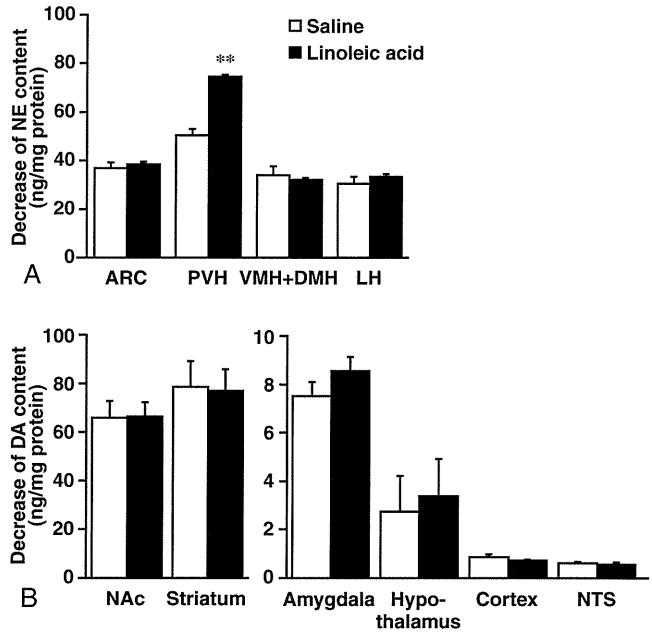

Fig. 5 – Jejunal linoleic acid infusion increases NE turnover in the PVH. Linoleic acid (100 μL/h) or saline was infused into the jejunum from −1 to 3 h in rats. α-MT (300 mg/kg, ip) was injected at 0 h. The NE and DA contents in the brain tissues were measured at 0 and 3 h after the α-MT injection. The NE and DA turnovers were assessed based on the decreases in the tissue monoamine contents. The results are expressed as the means±SEM of six rats per group. **P<0.01 vs saline infusion by Student's t test.

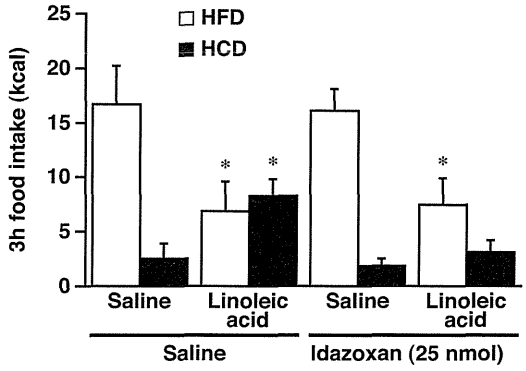

Fig. 6 – Intracerebroventricular injection of the α2-AR antagonist idazoxan suppresses the increase in HCD intake caused by jejunal linoleic acid infusion. Idazoxan (25 nmol) was injected into the third ventricle in rats implanted with a cerebral cannula at −1 h, followed by jejunal linoleic acid infusion. The HFD and HCD intakes were determined at 3 h. The results are expressed as the means ± SEM of seven rats per group. *P < 0.05 vs saline infusion by Student's *t* test.

jejunal linoleic acid infusion at 100 μL/h (Fig. 6). Administration of idazoxan (25 nmol) into the third ventricle suppressed the increase in HCD intake induced by jejunal linoleic acid infusion, but not affect the decrease in HFD intake. Idazoxan did not alter the HFD and HCD intakes in the control rats. The similar results were obtained by the 12.5 nmol dose of idazoxan (data not shown).

4. Discussion

We have revealed that intestinal infusion of long-chain fatty acids suppressed HFD intake in a dose-dependent manner, while HCD intake rather increased with the middle infusion dose (100 μL/h) and decreased to the control level with the higher infusion doses. A medium-chain fatty acid did not affect on feeding when infused into the jejunum. Linoleic acid infusion dose-dependently increased plasma GLP-1, PYY and CCK levels in the portal vein. Subdiaphragmatic vagotomy or midbrain transection prevented the changes in food preference and total calorie intake induced by linoleic acid infusion. Jejunal linoleic acid infusion increased NE turnover in the PVH. An icv injection of an α2-AR antagonist suppressed the increased HCD intake in response to linoleic acid infusion, but did not affect the decrease in HFD intake. These findings suggested that intestinal long-chain fatty acids modulated food preference as well as total calorie intake *via* the vagal nerve and midbrain–hypothalamic neural pathways. Furthermore, the effects of the α2-AR antagonist on the HCD and HFD intakes suggested that the brain distinctly controlled the HCD and HFD intakes after jejunal linoleic acid infusion.

In a two-bottle preference test, rodents show a greater appetite for long-chain fatty acids than triglycerides and medium-chain fatty acids [1,35]. Long-chain fatty acids seem to be the chemical cue involved in the orosensory perception of dietary lipids and regulation of fat preference. Oral lipid perception increases attraction to preferable fatty foods by activating mesolimbic reward circuits [26,27]. The lipid-binding protein CD36 [35] and two G-protein coupled receptors, GPR40 and GPR120 [36], are distributed across the lingual taste buds and play major roles in orosensory perception of long-chain fatty acids and fat preference. Present study showed that direct infusion of long-chain fatty acids into the jejunum selectively decreased HFD intake in a dose-dependent manner (Fig. 1A). As shown in Fig. 1C, jejunal linoleic acid (18:2) infusion reduced total calorie intake with the higher doses (150 and 200 μL/h), consistent with the previous reports [37,38]. However, when we examined the HCD and HFD intake individually, jejunal long-chain fatty acid infusion reduced HFD intake dose-dependently, while HCD intake increased with the middle dose of the infusion we examined (Fig. 1A and B). Protein intake was decreased with the higher infusion rates, similar to the total calorie intake (Fig. 1E). Alpha-linolenic acid (18:3) infusion altered the food preference and total calorie intake in the same manner as linoleic acid (Fig. 2A). Thus, while the increase in HCD intake did not show the dose–response manner, we understood that jejunal fatty acid infusion increased HCD intake but it was suppressed at the higher doses as a consequence of the suppression of total calorie intake.

Fatty acids in the small intestine stimulate the release of gut hormones such as CCK, GLP-1 and PYY [12,13], and these gut hormones transmit satiety signals to the brain *via* the vagal pathways [18,39,40] as well as through the bloodstream. We showed that jejunal linoleic acid infusion dose-dependently increased the plasma GLP-1, PYY and CCK levels in the portal vein (Fig. 3). The suppression of the total calorie intake with the higher infusion doses (≥150 μL/h) was correlated with increases in the plasma levels of anorectic gut hormones in the portal vein. These results suggested that gut hormones might be involved in the suppression of the total calorie intake.

PVH is highly innervated by noradrenalin-containing terminals and expresses α2-AR abundantly [41]. PVH neurons give rise to descending fibers which function to inhibit food intake [42]. Alpha2-AR is linked to Gi protein which inhibits neuronal activity. Therefore, NEs released by intestinal fatty acid infusion in the PVH access to α2-AR and then inactivates PVH inhibitory neurons, resulting in feeding. Leibowitz et al reported that NE injection into the PVH preferentially increases carbohydrate intake with little change in protein or fat intake *via* the α2-AR signaling pathway [24,25]. Consistent with these findings, our study revealed that jejunal linoleic acid infusion increased NE turnover in the PVH, and administration of the selective α2-AR inhibitor idazoxan into the third ventricle suppressed HCD intake but did not affect the decrease in HFD intake induced by jejunal linoleic acid infusion (Fig. 6). Our results suggested that α2-AR signaling in the brain, probably including the PVH, is involved in the HCD intake increase induced by jejunal long-chain fatty acid infusion. Further investigations are necessary to determine the sensing mechanism and chemical mediator at the intestinal level induced by jejunal long-chain fatty acid infusion for food preference regulation. In addition, we need to determine the important chemicals and nutrients in the HFD and HCD, including fats and carbohydrates, which are necessary for the food preference changes.

In conclusion, food preference, as well as total calorie intake, is modulated by intestinal long-chain fatty acid infusion through the vagal afferent nerve and midbrain–hypothalamic neural pathways. The α2-AR signaling in the brain is involved in the increase in HCD intake in response to jejunal long-chain fatty acid infusion, but not the decrease in HFD intake. These findings indicate that the brain distinctly regulates HCD and HFD intakes in response to jejunal long-chain fatty acid infusion.

Author contributions

NO, HY, KW, YM and MN conceived the experimental plan and discussed data analysis and interpretation. NO, MI, TS and SO contributed to the data collection. NO, TS and YM supervised the experiments. MI performed the data analysis. NO wrote the manuscript. HY and YM revised the manuscript.

Funding

This work was supported by JSPS 22390190 and The Takeda Science Foundation grants to MN.

Acknowledgment

We would like to thank H. Iwatsuka for a critical review of our manuscript and R. Matsuura for technical assistance.

Conflict of interest

The authors have nothing to disclose.

REFERENCES

[1] Tsuruta M, Kawada T, Fukuwatari T, et al. The orosensory recognition of long-chain fatty acids in rats. Physiol Behav 1999;66:285-8.
[2] Takeda M, Imaizumi M, Fushiki T. Preference for vegetable oils in the two-bottle choice test in mice. Life Sci 2000;67: 197-204.
[3] Drewnowski A, Brunzell JD, Sande K, et al. Sweet tooth reconsidered: taste responsiveness in human obesity. Physiol Behav 1985;35:617-22.
[4] Mela DJ, Sacchetti DA. Sensory preferences for fats: relationships with diet and body composition. Am J Clin Nutr 1991;53:908-15.
[5] Gower BA, Goree LL, Chandler-Laney PC, et al. A higher-carbohydrate, lower-fat diet reduces fasting glucose concentration and improves β-cell function in individuals with impaired fasting glucose. Metabolism 2012;61:358-65.
[6] Powley TL, Phillips RJ. Gastric satiation is volumetric, intestinal satiation is nutritive. Physiol Behav 2004;82: 69-74.
[7] Newson B, Ahlman H, Dahlström A, et al. Ultrastructural observations in the rat ileal mucosa of possible epithelial "taste cells" and submucosal sensory neurons. Acta Physiol Scand 1982;114:161-4.
[8] Höfer D, Püschel B, Drenckhahn D. Taste receptor-like cells in the rat gut identified by expression of alpha-gustducin. Proc Natl Acad Sci USA 1996;93:6631-4.
[9] Raybould HE. Nutrient tasting and signaling mechanisms in the gut. I. Sensing of lipid by the intestinal mucosa. Am J Physiol 1999;277:G751-5.
[10] Furness JB, Kunze WA, Clerc N. Nutrient tasting and signaling mechanisms in the gut. II. The intestine as a sensory organ: neural, endocrine, and immune responses. Am J Physiol 1999;277:G922-8.
[11] Katz DB, Nicolelis MA, Simon SA. Nutrient tasting and signaling mechanisms in the gut. IV. There is more to taste than meets the tongue. Am J Physiol 2000;278:G6-9.
[12] Feltrin KL, Little TJ, Meyer JH, et al. Effects of intraduodenal fatty acids on appetite, antropyloroduodenal motility, and plasma CCK and GLP-1 in humans vary with their chain length. Am J Physiol 2004;287:R524-33.
[13] Feinle C, O'Donovan D, Doran S, et al. Effects of fat digestion on appetite, APD motility, and gut hormones in response to duodenal fat infusion in humans. Am J Physiol 2003;284: G798-807.
[14] Lilja P, Wiener I, Inoue K, et al. Release of cholecystokinin in response to food and intraduodenal fat in pigs, dogs and man. Surg Gynecol Obstet 1984;159:557-61.
[15] Lin HC, Chey WY. Cholecystokinin and peptide YY are released by fat in either proximal or distal small intestine in dogs. Regul Pept 2003;114:131-5.
[16] Schwartz GJ, Fu J, Astarita G, et al. The lipid messenger OEA links dietary fat intake to satiety. Cell Metab 2008;8:281-8.
[17] Fu J, Gaetani S, Oveisi F, et al. Oleylethanolamide regulates feeding and body weight through activation of the nuclear receptor PPAR-alpha. Nature 2003;425:90-3.
[18] Smith GP, Jerome C, Cushin BJ, et al. Abdominal vagotomy blocks the satiety effect of cholecystokinin in the rat. Science 1981;213:1036-7.
[19] Date Y, Murakami N, Toshinai K, et al. The role of the gastric afferent vagal nerve in ghrelin-induced feeding and growth hormone secretion in rats. Gastroenterology 2002;123:1120-8.
[20] Angelopoulos N, Goula A, Tolis G. Current knowledge in the neurophysiologic modulation of obesity. Metabolism 2005;54: 1202-17.
[21] Cox JE, Kelm GR, Meller ST, et al. Suppression of food intake by GI fatty acid infusions: roles of celiac vagal afferents and cholecystokinin. Physiol Behav 2004;82:27-33.
[22] Agostoni E, Chinnock JE, De Daly MB, et al. Functional and histological studies of the vagus nerve and its branches to the heart, lungs and abdominal viscera in the cat. J Physiol 1957;135:182-205.
[23] Narayanan NS, Guarnieri DJ, DiLeone RJ. Metabolic hormones, dopamine circuits, and feeding. Front Neuroendocrinol 2010;31:104-12.
[24] Leibowitz SF, Brown O, Tretter JR, et al. Norepinephrine, clonidine, and tricyclic antidepressants selectively stimulate carbohydrate ingestion through noradrenergic system of the paraventricular nucleus. Pharmacol Biochem Behav 1985;23: 541-50.
[25] Leibowitz SF, Weiss GF, Yee F, et al. Noradrenergic innervation of the paraventricular nucleus: specific role in control of carbohydrate ingestion. Brain Res Bull 1985;14: 561-7.
[26] Liang NC, Hajnal A, Norgren R. Sham feeding corn oil increases accumbens dopamine in the rat. Am J Physiol 2006;291:R1236-9.
[27] Sahr AE, Sindelar DK, Alexander-Chacko JT, et al. Activation of mesolimbic dopamine neurons during novel and daily limited access to palatable food is blocked by the opioid antagonist LY255582. Am J Physiol 2008;295:R463-70.

[28] Brenner L, Yox DP, Ritter RC. Suppression of sham feeding by intraintestinal nutrients is not correlated with plasma cholecystokinin elevation. Am J Physiol 1993;264: R972-6.
[29] Crawley JN, Kiss JZ, Mezey E. Bilateral midbrain transections block the behavioral effects of cholecystokinin on feeding and exploration in rats. Brain Res 1984;322:316-21.
[30] Date Y, Ueta Y, Yamashita H, et al. Orexins, orexigenic hypothalamic peptides, interact with autonomic, neuroendocrine and neuroregulatory systems. Proc Natl Acad Sci USA 1999;96:748-53.
[31] Terao A, Oikawa M, Saito M. Cytokine-induced change in hypothalamic norepinephrine turnover: involvement of corticotropin-releasing hormone and prostaglandins. Brain Res 1993;622:257-61.
[32] Minokoshi Y, Alquier T, Furukawa N, et al. AMP-kinase regulates food intake by responding to hormonal and nutrient signals in the hypothalamus. Nature 2004;428: 569-74.
[33] Paxinos G, Watson C. The rat brain in stereotaxic coordinates. 4th ed. San Diego: Academic Press; 1998.
[34] Sousa R, Halper J, Zhang J, et al. Effect of lactobacillus acidophilus supernatants on body weight and leptin express in rats. BMC Complement Altern Med 2008;8:5.
[35] Laugerette F, Passilly-Degrace P, Patris B, et al. CD36 involvement in orosensory detection of dietary lipids, spontaneous fat preference, and digestive secretions. J Clin Invest 2005;115:3177-84.
[36] Cartoni C, Yasumatsu K, Ohkuri T, et al. Taste preference for fatty acids is mediated by GPR40 and GPR120. J Neurosci 2010;30:8376-82.
[37] Cox JE, Tyler WJ, Randich A, et al. Suppression of food intake, body weight, and body fat by jejunal fatty acid infusions. Am J Physiol 2000;278:R604-10.
[38] Ogawa N, Yamaguchi H, Shimbara T, et al. The vagal afferent pathway does not play a major role in the induction of satiety by intestinal fatty acid in rats. Neurosci Lett 2008;433:38-42.
[39] Abbott CR, Monteiro M, Small CJ, et al. The inhibitory effects of peripheral administration of peptide YY(3-36) and glucagon-like peptide-1 on food intake are attenuated by ablation of the vagal-brainstem-hypothalamic pathway. Brain Res 2005;1044:127-31.
[40] Koda S, Date Y, Murakami N, et al. The role of the vagal nerve in peripheral PYY3-36-induced feeding reduction in rats. Endocrinology 2005;146:2369-75.
[41] Cunningham Jr ET, Sawchenko PE. Anatomical specificity of noradrenergic inputs to the paraventricular and supraoptic nuclei of the rat hypothalamus. J Comp Neurol 1988;274: 60-76.
[42] Wellman PJ, Davies BT, Morien A, et al. Modulation of feeding by hypothalamic paraventricular nucleus alpha 1- and alpha 2-adrenergic receptors. Life Sci 1993;53:669-79.

Ghrelin Treatment of Cachectic Patients with Chronic Obstructive Pulmonary Disease: A Multicenter, Randomized, Double-Blind, Placebo-Controlled Trial

Keisuke Miki[1]*, Ryoji Maekura[1], Noritoshi Nagaya[2], Masamitsu Nakazato[3], Hiroshi Kimura[4], Shinsuke Murakami[4], Shunsuke Ohnishi[2], Toru Hiraga[1], Mari Miki[1], Seigo Kitada[1], Kenji Yoshimura[1], Yoshitaka Tateishi[1], Yasuji Arimura[3], Nobuhiro Matsumoto[3], Masanori Yoshikawa[4], Kenichi Yamahara[2], Kenji Kangawa[5]

1 Department of Internal Medicine, National Hospital Organization Toneyama National Hospital, Toyonaka, Japan, **2** Department of Regenerative Medicine, National Cerebral and Cardiovascular Center Research Institute, Suita, Japan, **3** Department of Neurology, Respirology, Endocrinology and Metabolism, Internal Medicine, Faculty of Medicine, University of Miyazaki, Miyazaki, Japan, **4** Second Department of Internal Medicine, Nara Medical University, Kashihara, Japan, **5** Department of Biochemistry, National Cerebral and Cardiovascular Center Research Institute, Suita, Japan

Abstract

Background: Pulmonary cachexia is common in advanced chronic obstructive pulmonary disease (COPD), culminating in exercise intolerance and a poor prognosis. Ghrelin is a novel growth hormone (GH)-releasing peptide with GH-independent effects. The efficacy and safety of adding ghrelin to pulmonary rehabilitation (PR) in cachectic COPD patients were investigated.

Methodology/Principal Findings: In a multicenter, randomized, double-blind, placebo-controlled trial, 33 cachectic COPD patients were randomly assigned PR with intravenous ghrelin (2 μg/kg) or placebo twice daily for 3 weeks in hospital. The primary outcomes were changes in 6-min walk distance (6-MWD) and the St. George Respiratory Questionnaire (SGRQ) score. Secondary outcomes included changes in the Medical Research Council (MRC) scale, and respiratory muscle strength. At pre-treatment, serum GH levels were increased from baseline levels by a single dose of ghrelin (mean change, +46.5 ng/ml; between-group $p<0.0001$), the effect of which continued during the 3-week treatment. In the ghrelin group, the mean change from pre-treatment in 6-MWD was improved at Week 3 (+40 m, within-group $p=0.033$) and was maintained at Week 7 (+47 m, within-group $p=0.017$), although the difference between ghrelin and placebo was not significant. At Week 7, the mean changes in SGRQ symptoms (between-group $p=0.026$), in MRC (between-group $p=0.030$), and in maximal expiratory pressure (MEP; between-group $p=0.015$) were better in the ghrelin group than in the placebo group. Additionally, repeated-measures analysis of variance (ANOVA) indicated significant time course effects of ghrelin versus placebo in SGRQ symptoms ($p=0.049$) and MEP ($p=0.021$). Ghrelin treatment was well tolerated.

Conclusions/Significance: In cachectic COPD patients, with the safety profile, ghrelin administration provided improvements in symptoms and respiratory strength, despite the lack of a significant between-group difference in 6-MWD.

Trial Registration: UMIN Clinical Trial Registry C000000061

Citation: Miki K, Maekura R, Nagaya N, Nakazato M, Kimura H, et al. (2012) Ghrelin Treatment of Cachectic Patients with Chronic Obstructive Pulmonary Disease: A Multicenter, Randomized, Double-Blind, Placebo-Controlled Trial. PLoS ONE 7(5): e35708. doi:10.1371/journal.pone.0035708

Editor: Christian Taube, Leiden University Medical Center, The Netherlands

Received December 9, 2011; **Accepted** March 20, 2012; **Published** May 1, 2012

Funding: Funding was from the Research Grant from the Ministry of Health, Labour and Welfare in Japan; the Program for Promotion of Fundamental Studies in Health Sciences of the National Institute of Biomedical Innovation (NIBIO) of Japan; the Takeda Scientific Foundation in Japan; and Health and Labour Sciences Research Grants, Clinical Research, H20-translational research-general-002. The funders had no role in study design, data collection and analysis, decision to publish, or preparation of the manuscript.

Competing Interests: The authors have declared that no competing interests exist.

* E-mail: mikisuke@toneyama.go.jp

Introduction

Pulmonary cachexia is common in the advanced stage of chronic obstructive pulmonary disease (COPD), and it is an independent risk factor for death in such patients [1,2]. Based on the notion that advanced COPD affects the whole body and causes wasting syndromes, many different therapeutic approaches have been attempted to improve this syndrome [1,3].

Pulmonary rehabilitation (PR) including exercise training is well accepted to improve exercise performance and quality of life in COPD patients [4], and it has been regarded as a nutritional adjunct therapy [5].

During the 1970s and 1980s, many gut peptides were identified [6]. Ghrelin, first discovered in 1999 as a novel growth hormone (GH)-releasing peptide isolated from the stomach, has been identified as an endogenous ligand for GH secretagogue receptor

[7]. Ghrelin also has a variety of GH-independent effects, such as causing a positive energy balance and weight gain by decreasing fat utilization [8], stimulating food intake [9], and inhibiting sympathetic nerve activity [10,11]. In addition, plasma ghrelin levels were elevated in cachectic COPD patients and were associated with the cachectic state and pulmonary function abnormalities, suggesting that endogenous ghrelin increased to compensate for the cachectic state and may provide important clues to improve the catabolic-anabolic imbalance in such patients[12]. In an open-label pilot study, we showed that ghrelin treatment increased walking distance in cachectic COPD patients [13]. Based on the above available evidence, a multicenter, randomized, double-blind, placebo-controlled study was conducted to test the hypothesis that the addition of ghrelin treatment to PR might benefit cachectic COPD patients. The objectives were to investigate the efficacy and safety of adding ghrelin to PR in cachectic COPD patients.

Methods

The protocol for this trial, supporting CONSORT checklist, and Supplementary Methods are available as supporting information; see Protocol S1, Checklist S1, and Supplementary Methods S1.

Study Design and Patients

The study was a 3-week, multicenter, randomized, double-blind, placebo-controlled trial of ghrelin administration during PR. The study was finally conducted at four clinical centers (National Cerebral and Cardiovascular Center, Miyazaki University School of Medicine, Nara Medical University, and National Hospital Organization Toneyama National Hospital) in Japan from September 2005 through May 2009, because Graduate School of Medicine, Osaka City University did not participate just before the start of the clinical trial. The study was conducted according to the Declaration of Helsinki and Good Clinical Practice guidelines and approved by the ethics committees of all participating study centers: The ethics committee of the National Cerebral and Cardiovascular Center (approval number, M17–13); The ethics committee of Miyazaki University School of Medicine (approval number, 218): The ethics committee of Nara Medical University (approval number, 05–012); and The ethics committee of the National Hospital Organization Toneyama National Hospital (approval number, 0311). All patients gave written

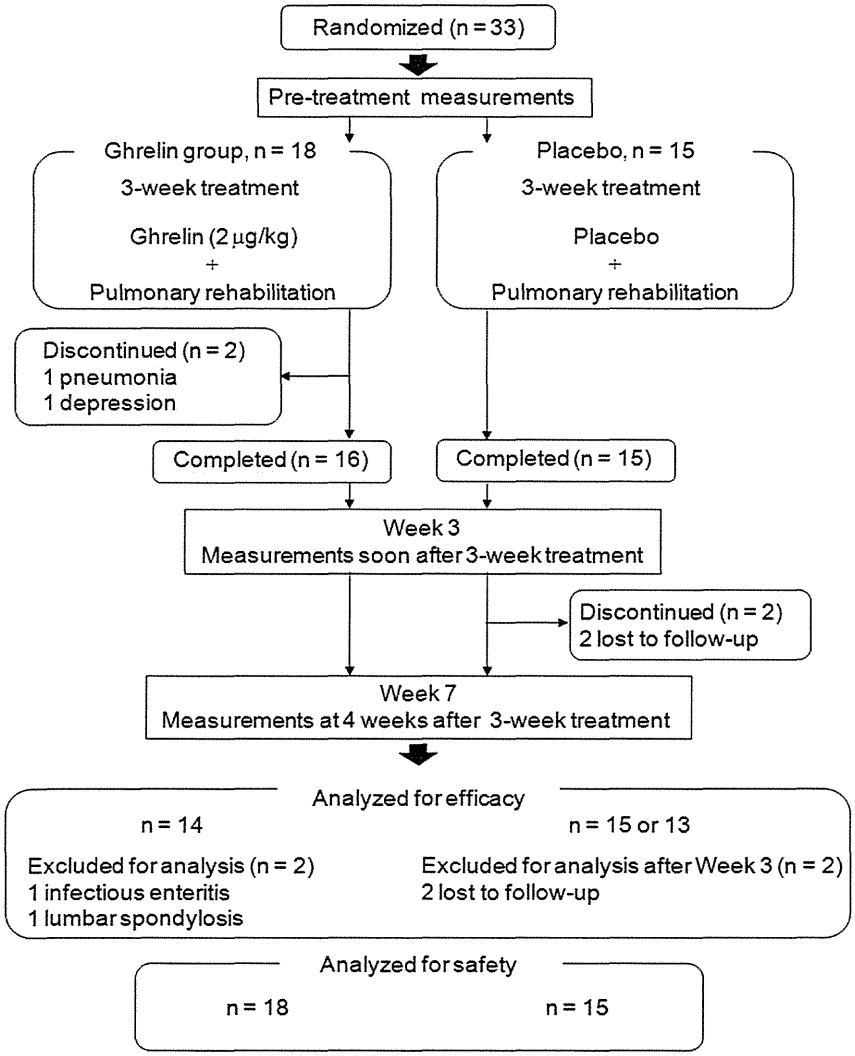

Figure 1. Trial profile.
doi:10.1371/journal.pone.0035708.g001

informed consent (in Japanese). The inclusion criteria were as follows: 1) severe to very severe COPD (forced expiratory volume in one second (FEV1)/forced vital capacity (FVC) of less than 70% and FEV1 percent predicted of less than 50%); 2) underweight (body mass index (BMI)<21 kg/m^2); 3) clinically stable and able to participate in PR; 4) between 20 and 85 years old; and 5) signed the agreement for participation in this study. Participants were excluded for any of the following: 1) malignant tumors; 2) active infection; 3) severe heart disease; 4) hepatic dysfunction (serum aspartate aminotransferase and alanine aminotransferase levels at least twice the upper limit of normal); 5) renal dysfunction (serum creatinine levels ≥2.0 mg/dl); 6) asthma; 7) definitely or possibly pregnant; 8) change in drug regimen within 4 weeks before participation in this study; or 9) judged to be unable to participate in this study by their physician. This study was registered with UMIN (University Hospital Medical Information Network in Japan: http://www.umin.ac.jp/ctr/), number C000000061.

Randomization and Interventions

Randomization was done in each center considered as a block. The randomization list was generated by a statistician from Hamamatsu University School of Medicine and maintained there until the study was finished and unblinded. Neither the physicians nor the patients were aware of the treatment assignments. Patients who met the eligibility criteria were enrolled and randomly assigned in a 1:1 ratio to receive PR with either ghrelin (2 μg/kg) or placebo twice a day for 3 weeks in hospital. The administration of ghrelin (2 μg/kg, ghrelin solution with 10 ml saline) or placebo was done intravenously over 30 minutes at a constant rate and repeated twice a day for 3 weeks. Patients were tested at pre-treatment, Week 3 after start of ghrelin or placebo administration with PR, and Week 7 after start of ghrelin or placebo administration with PR, i.e., 4 weeks after the completion of the combination treatment (Figure 1).

Preparation of Human Ghrelin

Human ghrelin obtained from the Peptide Institute Inc. was dissolved in distilled water with 3.75% D-mannitol and sterilized as described previously [13]. Ghrelin was stored in 2-ml volumes, each containing 120 μg ghrelin. The chemical nature and content of the human ghrelin in vials were rarefied as described previously [13]. All vials were stored frozen at −30°C until the time of preparation for administration.

Table 1. Patients' baseline characteristics. *

	Ghrelin, n = 14	Placebo, n = 15	p value
Age, years†	70.5 (6.2), 63–80	73.9 (6.0), 63–82	0.15
Sex, male/female‡	13/1	13/2	1.00
BMI, kg/m^2†	18.6 (2.1), 14.4–20.9	18.0 (2.1), 14.7–20.9	0.38
Cigarette smoking, pack years†	62.0 (30.9), 3.8–125	52.5 (28.8), 0.0–97.5	0.38
Pulmonary function†			
FEV1, L	0.78 (0.20), 0.54–1.21	0.77 (0.21), 0.47–1.21	0.90
%FEV1, % predicted	31.6 (8.1), 21.2–49.5	34.5 (9.1), 17.7–45.9	0.32
FEV1/FVC, %	38.0 (8.9), 24.6–50.5	38.8 (8.7), 25.4–52.9	0.74
VC, L	2.48 (0.37), 1.90–3.45	2.52 (0.50), 1.62–3.69	0.98
%VC, %	78.8 (9.3), 64.0–94.3	84.5 (12.6), 71.4–113.4	0.38
Exercise capacity on ICPET†			
Peak $\dot{V}o_2$, ml/kg/min	11.5 (3.3), 5.2–17.5	11.3 (3.5), 6.2–18.7	0.74
6-MWD, m†	328 (110), 148–619	315 (118), 85–498	0.84
SGRQ†			
Total score	58.2 (16.5), 36.3–84.4	50.2 (15.5), 21.3–77.3	0.23
Symptoms score	61.5 (22.5), 29.4–97.5	51.6 (19.8), 19.7–78.5	0.34
Activity score	72.5 (14.9), 41.7–92.5	65.9 (16.3), 35.3–92.5	0.34
Impacts score	46.7 (19.5), 20.0–84.4	39.2 (17.7), 9.4–69.7	0.53
Medications‡			
LAMA	9	6	0.27
SAMA	3	2	0.65
LABA	9	7	0.46
SABA	2	0	0.22
ICS	5	2	0.21
Methylxanthines	7	7	1.00

Data are presented as means (SD), and the minimum and maximum values unless otherwise stated. BMI = body mass index; FEV_1 = forced expiratory volume in one second; FVC = forced vital capacity; ICPET = incremental cardiopulmonary exercise testing; ICS = inhaled corticosteroids; LABA = long-acting β_2-agonist; LAMA = long-acting muscarinic antagonist; SABA = short-acting β_2-agonist; SAMA = short-acting muscarinic antagonist; VC = vital capacity.
*The groups shown represent only patients analyzed for efficacy. Medications are not mutually exclusive, and data are presented separately.
†Analyzed using a Wilcoxon rank sum test.
‡Analyzed using a Fisher's exact test.
doi:10.1371/journal.pone.0035708.t001